AN ABSTRACT OF THE THESIS OF

Julian A. Licata for the degree of Master of Science in Forest Science presented on December 19th, 2003.

Title: STRUCTURAL AND PHYSIOLOGICAL CHANGES WITH STAND AGE: Use of a Process-based Model to Compare Carbon and Water Fluxes in Young and Old-growth Douglas - fir / Western Hemlock Forest Stands.

Abstract approved:

Signature redacted for privacy.

Barbara J. Bond

Many studies have shown that net primary production in old-growth Douglas-fir/western hemlock forests is lower than in younger forests in similar sites, although the cause is still not clear. One possibility is that overall carbon assimilation, or GPP, is lower in older forests. However, it is difficult to measure GPP on an ecosystem scale, particularly in complex terrain where approaches such as eddy covariance are not possible. One approach is to use process models, although care must be taken to ensure that the model adequately represents "reality". I used a detailed soil-plant-atmosphere (SPA) continuum model, which explicitly links CO2 and H2O fluxes through stomatal conductance. The SPA model has multiple canopy and soil layers where the hydraulic system is modeled as analogue to an electrical circuit. The model accounts for many

structural and physiological differences in the stands. I carefully calibrated the model to accurately represent transpiration in a young (ca 25 years old) and an old-growth (ca 450 years old) Douglas-fir/western hemlock stands at Wind River, WA, based on detailed measurements of soil water depletion and sap flow and then used the model to predict variation in GPP among the sites.

The modeling approach of this study allowed me to perform sensitivity tests to examine the likely influence of individual structural and physiological parameters on transpiration and GPP. The variables tested were height, above ground leaf specific conductivity, capacitance, leaf area and root vertical distribution, minimum mid-day water potential, canopy water storage, rain interception, root resistivity, and photosynthetic capacity. Within the natural range of variation of these variables, the most influential of these on GPP and Transpiration was height, followed by above ground leaf specific conductivity, and minimum mid-day water potential. By identifying the sensitivity of water and carbon fluxes to the range of natural variation found in these variables, it was possible to examine the likelihood of various hypotheses proposed to explain the age-related decline in productivity.

Finally, I modified the model software in order to improve its versatility and make it available to other researchers for use in additional types of forests

STRUCTURAL AND PHYSIOLOGICAL CHANGES WITH STAND AGE:

Use of a Process-based Model to Compare Carbon and Water Fluxes in Young and Old-growth Douglas - fir / Western Hemlock Forest Stands.

by

Julian A. Licata

A THESIS

submitted to

Oregon State University

in partial fulfillment of

the requirements for the

degree of

Master of Science

Presented December 19, 2003

Commencement June 2004

Master of Science thesis of Julian A. Licata presented on December 19, 2003.

APPROVED:

Signature redacted for privacy.

Major Professor, representing Forest Science

Signature redacted for privacy.

Head of the Department of Forest Science

Signature redacted for privacy.

Dean of the Graduate School

I understand that my thesis will become part of the permanent collection of Oregon State University libraries. My signature below authorizes release of my thesis to any reader upon request.

Signature redacted for privacy.

Julian A. Licata, Author

ACKNOWLEDGEMENTS

This thesis is an integrating modeling study and would not have been possible without the help of many people. First, I would like to thank my major professor, Barbara Bond, for her assistance, support and wise advice throughout these years. Her help started before I actually started the graduate program. I met her in the southern lands of Patagonia, and since I mentioned to her that I would like to be one of her graduate students at OSU, she never stopped being a source of encouragement to continue (or start) my scientific career, and develop my ideas. She always knew the exact words to motivate me in those moments when everything seemed to be wrong. I would like to thank also my committee members Dominique Bachelet and Mike Unsworth for their support and advice.

I am grateful with the long distance, but prompt, support and advice of Mathew Williams, who originally developed the model I used in this study.

I want to thank all the researchers that have shared their results with me in order to feed the 'input-consumer' model I used for this study: Tom Pypker, Ken Bible, Julia Kerrigan, Jeff Klopatek, Jess Parker, Kate George, and Troy Ocheltree. A special thank to Jeff Warren, Rick Meinzer, Renee Brooks, and David Woodruff for their help in critical moments of this process. I am also grateful to Dave Shaw and all WRCCRF staff.

I appreciate the funding provided for this project by the Forest Science Department of Oregon State University, and by the Western Regional Center (WESTGEC) of the National Institute for Global and Environmental Change (NIGEC).

I sincerely appreciate the support, advice, and homely environment I found in the lab I was glad to work : Georgianne Moore, Nate Mc Dowell, Nicole Czarnomski, John Campbell, Steve Van Tuyl, and Jennifer Swenson. I want to thank Tom Pypker again, but not for sharing his results this time, but for his priceless help with a whole variety of issues that an international student can face specially during my first months here (i.e., checking the grammar of my writing, helping me with paperwork, etc.).

None of this would have been possible if not for the encouragement, support and love of my family and ex-girlfriend Elvira Erausquin. It was also very important the affection and support I received from my friends in Corvallis. A special thanks to Erika Adams, and Guido Corno for the mutal encouragement, help and discussions we had concerning our theses, politics, and life. Crucial for my last months' survival was the extra supply of yerba mate that J.C. Villars got especially for me from Portland.

TABLE OF CONTENTS

LIST OF FIGURES

LIST OF FIGURES (continued)

LIST OF FIGURES (continued)

Figure Page

LIST OF TABLES

STRUCTURAL AND PHYSIOLOGICAL CHANGES WITH STAND AGE:

Use of a Process-based Model to Compare Carbon and Water Fluxes in Young and Old-growth Douglas - fir / Western Hemlock Forest Stands.

Introduction

Global climate change has become a major concern in the scientific community over the last few decades. Human impacts on the global carbon cycle, and the potential feedbacks to climate, are being debated. Increased concentrations of carbon dioxide in the atmosphere are thought to be partially responsible for the greenhouse effect. Terrestrial ecosystems are a critical component of the global carbon budget (Cramer et al. 2001). Carbon assimilation through photosynthesis fixes atmospheric carbon dioxide. However, the balance between carbon uptake from photosynthesis and release from respiration, fires and other disturbances varies with climate, ecosystem type, and disturbance regime. Several studies have addressed the links between vegetation, climate, and disturbance regime to estimate carbon balance in different ecosystems (Sellers et al. 1997, Lawton et al. 2001, Bachelet 2003, Bonan et al. 2003, Lenton and Hungtinford 2003). It has been shown that seasonal climate (e.g., variations in growing-season length or cloudiness) can regulate seasonal and inter annual fluctuations of carbon uptake in forest ecosystems (Barford et al. 2001, Salesca et al. 2003). But there

is a lack of information about the processes involved in these interactions, and how the processes differ in forests of different ages.

Global, regional, and local hydrology are closely linked to the distribution and activity of vegetation (Williams et al. 2001). Because of the potential for changes in global climate, and thus patterns of precipitation, understanding the links between hydrology and plant processes is of great interest (Houghton 1996).

One approach for predicting ecosystem-scale storage and fluxes of carbon is to make measurements at scales below the level of the ecosystem in order to understand the mechanisms controlling carbon cycling. Measurements of leaf- and canopy-level carbon assimilation over the daily, seasonal, and annual time scale provide information that can be used to understand the links between environmental factors and physiological processes, which can then be scaled to estimate ecosystem fluxes. However, measurements of physiological processes are rarely made for large, old trees (Ryan and Yoder 1997). The common focus of physiological analysis on young rather than old trees is in large part due to the difficulty in accessing the canopies of old trees. The recent increase in the scientific use of towers, cranes, balloons and even airships, has augmented research of canopy processes in tall forests. These studies help to understand the mechanisms behind the decline in productivity through the succession of forest stands.

A decline in productivity of even-aged forest stands after achievement of maximum leaf area is commonly observed around the world. Although this pattern has been recognized for centuries, clear evidence for the mechanism causing this decline is still lacking (Birıkley et al. 2002, Ryan et al. 2003). Understanding causes and effects of this growth pattern is fundamental for determining the role of forests as sinks or sources of carbon under diverse scenarios (Ryan et al. 1997).

The first objective of this study was to adapt a computer simulation model of forest processes to a young (25year old) and an old-growth (450-500 year old) Douglas-fir/western hemlock forest stand in order to predict fluxes between them and the atmosphere. Measured values of water fluxes were used to calibrate the model.

The second objective was to use the calibrated model to estimate carbon fluxes and gross primary productivity. Although it is relatively easy to measure water fluxes in ecosystems, direct measurement of GPP is more difficult. Eddy covariance methods can be employed in some circumstances to measure carbon fluxes, but this approach is very expensive, and in any event the method is restricted to areas with uniform vegetation and flat topography.

The third objective was to use the model to quantify the effect of the variables found different between stands of different developmental stages on carbon and water fluxes.

The fourth and final objective was to improve the versatility of the model software and make it available to other researchers for use in additional types of forests.

The model, SPA ("Soil Plant Atmosphere") was developed in the late 1990s by Mathew Williams, now of the University of Edinburgh. As it now stands, the model is primarily used as a tool by Dr. Williams and a few students. Modifications of the model interface make it more accessible to other users.

Background

Modeling global climate change and plants-atmosphere interactions

Scientists first began paying attention to global climate change by the late 1980's. Interest focused primarily on the greenhouse effect produced by accumulation of excess CO2 in the atmosphere and the associated impacts on terrestrial ecosystems (Sellers et al. 1997). The impetus to understand and predict the storage of carbon in forest ecosystems worldwide has grown dramatically over the last decade (Baldocchi and Vogel 1996) in response to reports of increasing atmospheric CO_2. Nowadays, while the negotiations over the Kyoto protocol continue, the terrestrial sinks and sources of carbon continue to be controversial and several questions should be answered. How important are terrestrial sources and sinks in the global carbon cycle, and how may they change in the future

(Scholes and Noble, 2001)? To answer these questions it is necessary to understand the mechanisms behind the interactions between plant ecosystems and atmosphere. Understanding the processes will allow generation of models that would accurately predict the responses of the terrestrial system under changing conditions. Mechanistic models have the potential to be important tools for policy makers to predict possible consequences of political decisions and international treaties on greenhouse gas emissions and land use and management.

Some models developed to answer questions concerning the global carbon cycle evolved from the atmospheric general circulation models (AGCM), initially used for climate simulation and weather forecasting. These models required data on fluxes of radiation, heat, water vapor, and momentum across the land-atmosphere interface. To get more accurate inputs for these items, the latest generation of these models included dynamic vegetation sub-models that can be directly responsive to changes in climatic conditions and atmospheric CO_2 (Sellers 1997).

With the current high rate of CO_2 increase in the atmosphere, the need for realistic and accurate models becomes more urgent (Sellers et al. 1997). Because of the very large and highly variable exchange of carbon between the atmosphere and forest ecosystems, understanding how age-related changes in structure and functions in forest stands varies through the succession of forest

ecosystems is crucial to increase the accuracy of model predictions (Lenton and Huntingford 2003).

The model selected for analyses in this thesis is the soil-plant-atmosphere (SPA) continuum model (Williams et al. 1996). The SPA model is unique in explicitly inter-relating water and carbon dioxide fluxes by stomatal conductance behavior under different stimuli. It is especially appropriate as a tool to analyze processes in different stages of forest development because it explicitly couples the hydraulic path of water through soil and vegetation to stomatal activity, thus linking forest structure to carbon and water exchange. It uses a detailed physiological approach, with a time step of thirty minutes. The SPA model has been applied to several ecosystems (Williams et al. 1996, Law et al 2001, and Williams et al. 2001), and has been demonstrated to be an appropriate model for different C_3 plant ecosystems.

The SPA Model

The SPA model is a multiple layer process-based model, where the structure of the canopy is divided into 10 layers to represent the vertical variation of the physical environment and leaf biochemical features (Williams et al. 1996, Law et al 2001, and Williams et al. 2001). The soil-roots sub-model has 20 layers, allowing a detailed representation of root distribution in depth.

The SPA model uses a pipe hydraulic scheme approach, assuming that each canopy layer is served by an independent water supply system of roots. It employs an unbranched hydraulic pathway scheme, using an electric circuit analogy approach. Every 30 minutes the absorption of photosynthetically active radiation (PAR) and other wavelengths, leaf boundary layer conductance, and soil water availability are determined for each canopy layer. Leaf water potential varies with transpiration, which is calculated by the Penman-Monteith equation. The variation of leaf photosynthetic capacity parameters changes with foliar nitrogen distribution among canopy layers

The key hypothesis governing the biological components of the model is that stomatal conductance (g_s), is controlled to maximize carbon gain per unit nitrogen (N) within the limits set by the rate of water uptake and canopy water storage.

(For a more detailed description refer to the Methods section.)

Previous applications of the SPA model

The original model was developed and successfully applied in a temperate deciduous forest of *Quercus rubra* and *Acer rubrum* at Harvard Forest in central Massachusetts, USA. It showed a strong correlation between predicted hourly $C0_2$ exchange rate ($r^2 = 0.86$) and latent energy (LE; $r^2 = 0.87$) with independent eddy correlation measurements (Williams et al. 1996). Later, the model was

applied to investigate the seasonality of carbon and energy exchange in a tropical rainforest in Brazil (Williams et al. 1998). The authors concluded that an increase in the soil-root hydraulic resistance in the dry season introduced a significant seasonal cycle to carbon and water fluxes for that tropical forest (Williams et al. 1998). The model was also applied to multiple land cover types in the arctic tundra to explore the dynamics of net ecosystem production (NEP) at sites with widely differing vegetation structure and moss/lichen cover (Williams et al.2000).

More recently, the model was applied in two ponderosa pine stands. To get a better fit with the eddy correlation data, a detailed belowground component was added to the model. These allowed the model to account for seasonal soil water constraints (Law et al. 2000, Williams et al. 2001). Nevertheless, the goodness of fit was lower than in the temperate deciduous forest that had minimal water constraints during the growing season. The modified model could explain only 63% of the daily variance in LE, and 66% of gross primary production. In another study in ponderosa pine, a "single tree" version of the model was applied to investigate patterns of whole-tree sapflow in trees of different size and age (Williams et al. 2001). Three hypothetical controls on hydraulic resistance were tested using the "single tree" version of the model. The hypothesis that gave the most effective explanation of the variation in sapflow was able to explain up to 90% of the variance in sapflow.

Age-related decline in forest stands

It is widely accepted among foresters and forest scientists alike, that an even-aged forest will continuously increase the net primary productivity (NPP) until canopy closure, and then productivity will start to decline. However, the mechanisms behind this decline remain unclear (Battaglia 2001, Ryan et al. 2003). The classic explanation for this decline was that photosynthesis, or gross primary productivity (GPP), remains constant as leaf area stops increasing, and subsequent increases in the amount of biomass leads to an increase in respiration (fig.1.1). This explanation has been accepted though decades without a rigorous evaluation against empirical evidence (Binkley et al. 1995, Ryan et al. 1997, Ryan et al. 2003). Recent studies have shown that there is a decline in net photosynthesis as stands age, or individual trees grow taller (Yoder et al. 1994, Hubbard al.1999). Also, there is experimental evidence that does not support the increasing respiration hypothesis as the cause of growth decline (Ryan and Waring 1992). It has been found that respiration is more related to growth than to biomass accumulation (in other words, respiration tends to function more as a response variable – increasing with increased growth – than as a causal factor in varying rates of biomass

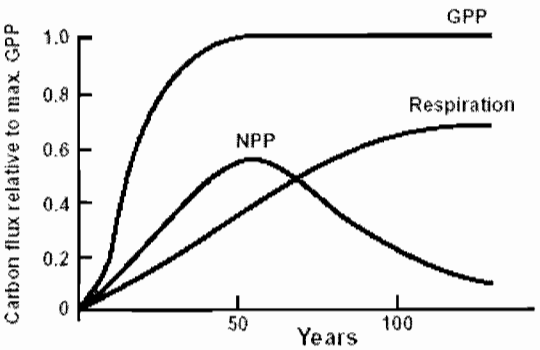

Figure 1.1 - From Ryan et al. (2003) after Barnes et al. (1998). Reinterpretation of the classic hypothesis of age-related decline in stand productivity.

accumulation). The ratio GPP to respiration is conservative over a wide range of plants sizes (Gifford 2001). Ryan et al. (1997) proposed an alternative model of carbon fluxes through stand development where the respiration is a relative constant fraction of GPP (fig.1.2). However, the reasons for the reductions in GPP were not demonstrated to be caused by a simple mechanism.

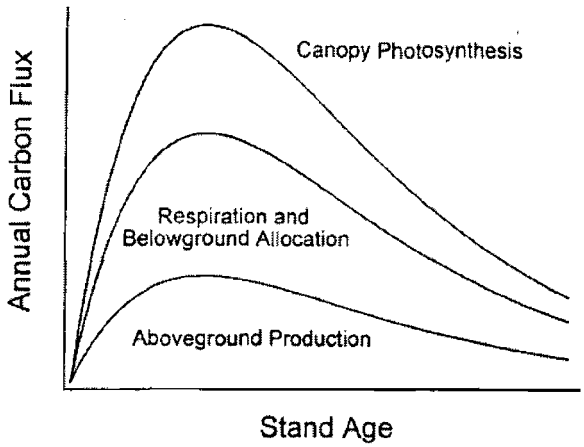

Figure 1.2 - From Ryan et al. (1997) Proposed model of carbon fluxes through stand development.

A variety of alternative hypotheses were proposed to explain the age-related decline in productivity:

1) Hydraulic limitation hypothesis. As height increases, leaf specific hydraulic conductance (k_l) and stomatal conductance(g_s) decline, and thus, carbon assimilation decreases (Yoder et al. 1994, Ryan and Yoder 1997,). The rationale supporting this hypothesis as stated by Barnard and Ryan (2003) is:

i. Stomata must close to regulate leaf water potential and to avoid xylem embolism.

ii. Hydraulic resistance increases with path length, being enhanced with increasing height by the effect of gravity.

iii. Stomata closure will occur for longer periods of time in larger trees, and thus overall stomatal conductance must decrease.

iv. Photosynthesis must be reduced as a result of lower stomatal conductance.

v. Reduced photosynthesis must be sufficient to account for reduced growth.

Several studies have been conducted to test this hypothesis (Hubbard et al. 1999, McDowell et al. 2002b, Phillips et al. 2002, Barnard and Ryan 2003) and provided evidence to support the tenets enumerated above. However, most of the studies found that the decrease in photosynthesis could not fully explain the

decline in productivity. Several compensatory mechanisms were proposed as a way to reduce the hydraulic constrains imposed by the increase in height or path length.

There is evidence to support the hydraulic compensation of large trees. In old-growth Douglas-fir trees a change in the leaf to sapwood area ratio lead to an increase in leaf specific conductivity(McDowell 2002a). Many tree species have a midday minimum leaf water potential (ψ_{lmin}) threshold that would prevent xylem embolism (Jones and Sutherland 1991, Bond and Kavanagh 1999). A decrease of the threshold ψ_{lmin} was also found in Douglas fir trees as they grow taller/older (fig. 1.3). Having a lower ψ_{lmin} would allow the plant to have stomata open for longer periods of time, and thus, increase the overall photosynthesis (Hubbard et al. 1999, McDowell 2002b, Phillips et al. 2002).

Increase in capacitance, or stored water capacity, with height has been also proposed as a compensatory mechanism for hydraulic limitations in large trees (Phillips et al. 2003). Capacitance is defined as the ratio of change in tissue water content to the change in water potential. In other words, a greater capacitance would allow the plant to lose water without changing the water potential of the tissues. The use of stored water would allow leaves to maintain stomata open for longer periods of time, thus increasing the possibility of carbon gas exchange. Phillips et al. (2003) found evidence of increased use of stored water in larger trees of Douglas-fir, Oregon white oak, and ponderosa pine.

Other compensatory mechanisms for hydraulic constraints, like increased fine roots to foliage ratio or increased xylem permeability, have been proposed (Mencuccini and Magnani 2000).

Although most of the studies found some kind of the compensatory mechanism for the potential increases in hydraulic resistance with increased height, none of them found total compensation, disproving the hypothesis of hydraulic homeostasis with age (e.g., Becker et al. 2000). However, the hydraulic limitation hypothesis did not explain completely the productivity decline in forest stands.

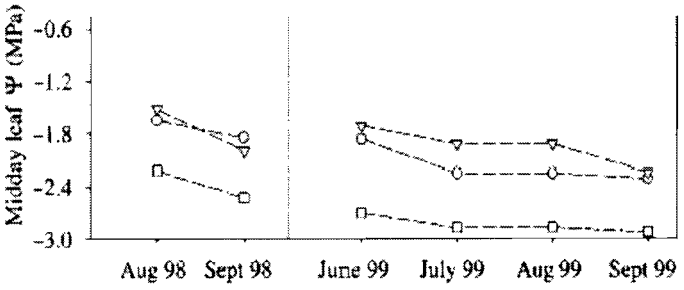

Figure 1.3 – From Phillis et al. (2002). Monthly mean of midday ψ_{lmin} of 15-m (○), 32-m (▽) and 60-m (□) Douglas-fir trees.

2) Nutrient immobilization. The availability of nutrients may decrease as they accumulate in biomass (Binkley et al. 1995). As wood has a low nitrogen to carbon ratio, its accumulation in old-growth stands may immobilize nitrogen from throughfall, N-fixation, and soil reserve sources. Photosynthetic capacity has been shown to be closely related to nitrogen nutrition. Then, nitrogen immobilization may produce a reduction in photosynthesis and consequently in productivity. However, evidence from field measurements was variable (Battaglia 2001); although nutrient immobilization may augment age-related productivity decline in some forests, it cannot explain the growth decline for all forests.

3) Allocation changes. Magnani et al. (2000) suggested that an increase in the proportion of photosynthate allocated belowground could explain part of the decline in productivity. This proposed as another mechanism to compensate for height-related hydraulic constraints. According to this hypothesis, carbon is partitioned into above- versus below-ground components to optimize the marginal costs of maintaining adequate root and stem hydraulic conductance. The increase of fine root biomass would lead to an increase root turnover and, consequently, increase respiration. However, this belowground carbon allocation occurs later in the stand development than the decrease in productivity, so it is not a viable explanation for the reduced productivity that coincides with stand closure. In addition, a more recent study (Matamala et al. 2003) suggested that fine root production and turnover in forests have been overestimated.

4) Increased allocation to reproductive structures has also been proposed as a cause of the reduction in wood production (Ryan et al. 1997 after Linder and Troeng 1981). However, the energy used in production of reproductive structures varies hugely over 5 to 10 year cycles in most trees, .Growth, on the other hand, is sensitive to year-to-year variations in weather, but does not vary on the same periodic cycles as reproduction.

5) Genetic maturation of meristems. Genetic expression on meristems may change with tissue age and cell divisions (Ryan et al. 1997 after Greenwood and Hutchinson 1993). Grafted scions from mature trees into young trees kept on

growing with mature traits. Nevertheless, the causes and consequences of age-related genetic expression remain unclear.

In this study I am using a modeling approach that allowed me to quantify the individual impact of structural and physiological variables found to be different between the young and the old-growth stands of Douglas-fir/western hemlock forest. By identifying the sensitivity of water and carbon fluxes to the range of natural variation found in these variables, it is possible to examine the likelihood of the various hypotheses presented above. However, more attention was given to the hydraulic limitation hypothesis.

.

Methods

In this modeling study, an existing process-based model was adapted to two Douglas-fir stands of different developmental stages at the Wind River Canopy Crane Research Facility (WRCCRF). Permanent sampling plots were established prior to this study as part of a larger research project led by Dr. Barbara Bond. Other researchers are using these plots for a variety of other studies. Results from these other investigations were used to parameterize and test the performance of the model. The adaptation of the model can be divided into two parts: 1) The parameterization of the model, where the logical and mechanistic structure was not modified and was tested for fit against independent field data; and 2) The modification of the model logical structure, adjusting algorithms that were originally developed for different ecosystems. During the adaptation process, I found that it was impossible to parameterize the model without modifying the source code of the program, which was written in Fortran 90/95. Therefore, I transformed the original program code and added new features. These changes will allow future users of the model to parameterize the model without having to deal with the Fortran programming code. I also added a new sensitivity analysis algorithm and other input/output features, which are described below, to the program in order to increase its functionality.

Description of the area

The WRCCRF is a cool, moist, Douglas-fir/western hemlock forest located in the southern Cascade Range of Washington State. Weather data from the Wind River Ranger Station (approximately 3 km distant) are characteristic of a temperate winter wet, summer dry climate with 2528 mm of annual precipitation, less than 10% occurring between June and September. Average annual snowfall is 2330 mm. Mean annual temperature is 8.7 degrees C. Local geology is characterized by volcanic rocks and deposits of Miocene/Oligocene and Quaternary age, as well as intrusive rocks of Miocene age. Soils are generally deep, well drained, stone free, and derived from volcanic tephra, loams and silt loams. The vegetation is transitional between the Western Hemlock Zone and the Pacific Silver Fir Zone Plant Associations. There is a patchy distribution pattern of different forest stand ages through the landscape with most of the old growth forest patches being smaller than 50ha (Lehmkuhl et al. 1991). A complete description of the WRCCRF is provided in Shaw et al. (in press).

Description of the sites

The model was parameterized for two Douglas-fir/western hemlock stands of different age, an old-growth (450-500 years old) and a young (25 years old) stand. The old-growth stand was located in a flat terrain near the base of Trout

Creek Hill, an extinct volcanic cone (45°49'13.76" N, 121°57' 06.88" W), at an elevation of 368 m.

A seasonally intermittent stream runs approximately at 150m from the study site, and the water table reached up to 1.7m deep at the beginning of the summer. There are eight conifer species with an average stand density of 429 stems/ha. The basal area of the forest is 82.8 m^2/ha. Average height of Douglas-fir is 52.2 m (tallest tree is 64.6 m), while western hemlock averages 19.4 m (tallest tree is 55.7 m). The forest composition is slowly shifting from dominance by Douglas-fir to western hemlock, western red cedar, Pacific yew, and Pacific silver fir (see table 1). The understory vegetation is dominated by vine maple, salal, and Oregon grape. Well-developed epiphytic communities of lichens (1.3 metric tons/ha) and bryophytes are present in the complex and multi-layered canopy (see Shaw et al., in press, for more details).

% of total Leaf Area		
Species	**Old Growth [1]**	**Young [2]**
Douglas-fir	28	91.8
W.Hemlock	40	5.1
W.R.Cedar	15	0.0
Vine Maple	4.4	2.6
Yew	1.2	0.0
Pacific Silver Fir	1.3	0.2
other spp.	10.1	0.2

Table 1 – Species leaf area contribution per site.
[1] Data from Thomas & Winner 2000
[2] Estimate from T. Ocheltree (unpublished data)

The young site is 6km west of the old-growth site (45°49'07.89" N, 121°59'38.95" W), located on a gentle hillslope at 473m elevation. The vegetation of this young site is primarily Douglas-fir with sparse trees of other species representing a minor component of the living biomass (see table 1, for leaf area composition of both sites).

Field Measurements

Meteorological data

Microclimatic information for the year 2002 was provided by Ken Bible from the WRCCRF Microclimate Monitoring Database. The SPA model runs on a 30-minute time step and requires a complete information of wind speed, air temperature, relative humidity (RH), photosynthetically active radiation (PAR) and precipitation at this temporal frequency. The first four of these variables were measured in a meteorological station located on the canopy crane tower at 60m above ground in the center of the old growth site. The measurement Equipment, Variable (Symbol) and Units were:

Campbell Sci. Inc., CR10 datalogger, scan rate 20 seconds; output 30 minutes

LiCor 190SB quantum sensor, photosynthetically active radiation (PAR) micromoles/s/m2

Vaisala HMP35C, air temperature (Ta) degrees C and relative humidity (RH) percent

Handar 425AH ultrasonic wind sensor, average and maximum wind speed (u, u_{max}) in m/s, direction (dir) and standard deviation (stdir) in degrees

Vaisala CS105 barometric pressure sensor (P) mb

The precipitation data were collected in a field station in an open field 700 meters S-SE of the canopy crane. The equipment used was a Texas Electronics TE525WS tipping bucket rain gauge.

Sap flux measurements

Estimates of the mean sap flux per unit ground area of two stands for the year 2002 was used to parameterize the SPA model. To calculate the average sap flux per unit ground area at the stand level, Granier-type sensors (Granier, 1987) were installed in several trees of the different species present on each site. Dr. Kate George (post doctoral associate for a related project) was in charge of the sites and trees selection, field measurements and data compilation, while I did the data "cleaning" and scaling analysis. At least two pairs of sensors per tree were installed at 1.4m height.

In the old-growth site, 46 pairs of sensors (each sensor is comprised of a reference and a heated thermocouple) were installed by Dr. George in

representative trees of the six most frequent species present in the site. For the purpose of this study, only 20 sensors of this site were used to calculate the mean sap flux density per unit ground area. Data from the rest of the sensors were not used due to sensor malfunctions for periods longer than 60 days during the growing season. The sensors used were installed in two dominant Douglas-fir, two medium sized and two small western hemlock, one large and one small western red cedar, two yew, one pacific silver fir and six vine maple trees. In addition to these data, I utilized sap flux data acquired by David Woodruff and Rick Meinzer from six large western hemlock trees in the same site. In the young site, 21 pairs of sensors were installed in the principal species present. The trees used to estimate the mean sapflow density per unit ground area of the stand were: two dominant Douglas-fir, two co-dominant Douglas-fir, two suppressed Douglas-fir, one co-dominant western hemlock, one small western hemlock and two vine maple.

Programs created to calculate, fill, and clean the sapflow data

Continuous sapflow data throughout the 2002 growing season were required to parameterize the model. However, due to power outages and sensor malfunctioning, there were numerous gaps and erroneous data present in the "raw" data collected in the field. In order to use the data as required, I developed a series of Fortran programs to delete dubious data and fill in the gaps based on a consistent set of criteria. The first program computes sapflow

from the mV output of the sensors, while the rest of the programs deal with data quality and continuity. A short description of the programs developed is given below.

Program 1: Computing sap flux density from raw mV data

This program transforms the mV data read from the sensors to sap flux density per sapwood area. The mV data are transformed to temperature difference in accordance to standard equations for copper-constantan thermocouples. Then sapflow density per sapwood area ($\bar{J}$, g m^{-2} s^{-1}) is calculated using the equations described by Granier (1987).

$$\bar{J} = 119 * K^{1.231} \quad (1)$$

where :

$$K = \frac{\Delta T_m - \Delta T}{\Delta T} \quad (2)$$

where:

ΔT_m = daily maximum temperature difference between the reference and the heated sensor in the sensor-pair

ΔT = instantaneous temperature difference

This program discarded measurements where any of the following conditions occurred:

The maximum temperature difference (ΔT_m) differed by 30 % or more from the averaged ΔT_m for the previous 10 days

The mV data were out of the specified range for that pair of thermocouples

ΔT was bigger than 25°C

The resulting sapflow density was out of a specified range (0-200 g m^{-2} s^{-1})

There was an instantaneous increment mV data greater than 0.05mV

The program also discarded a whole day of data if the number of peaks (i.e., local maxima) in the mV data for that day was over 1/4 of the total number of data for the day or 1/3 in the case of vine maple. The purpose of this criterion was to eliminate erratic data that are characteristic of malfunctioning sensors.

Program 2: Checking and correcting the decimal time

To compare the results of the model against the field data, the timesteps of the modeled and measured data must be the same. However, because the times recorded by the data logger for field data occasionally had missing timesteps, repeated data, or incorrect values, a program was written to check if the decimal time of the files was complete, and whenever there was an error, the

correct decimal time was calculated. If there was only one timestep missing, the columns were filled in with a linear interpolation between the previous and the next for each column. In the other cases, the columns were filled in with a gap indicator, which is a constant value notably different from good or acceptable data values (i.e., –999 in a file where the range of variation is usually between 0 and 1).

Program 3: Gap interpolator

The purpose of this program is to fill in small periods of data missing (2 hours at most for the sapflow data). In contrast with the program above that looks for erroneous or missing data in the decimal time, this one checks the completeness of the variable columns. It reads column by column (i.e., looking at data for specific sensors over time), searching for periods with gap indicator values or data out of a specified range. When the program finds a period with missing or bad data, it counts the number of timesteps of the gap, and if it is smaller than the threshold value specified in the options, it will fill in the missing timesteps with a linear interpolation between the last good previous value, and the first good next value.

Program 4: Gap proportional filler

One of the main problems with the sapflow sensor data was that most sensors had periods of missing data longer than two hours. These missing periods usually occurred at different times in different sensors. In addition, the total

number of each sensors installed in a particular species at each site was relatively small. Therefore, if not filling in missing values, mean values of sapflow density calculated from "good" sensors at any point in time would indicate artificial "shifts" in data as different sets of sensors were "up" (i.e., data were reliable), "down" (i.e., data were unreliable") and were subsequently repaired. This could be interpreted as a biological change when, in reality, it is just an artifact of sampling.

After applying the programs mentioned above, the periods of missing data longer than 2 hours were not changed. For missing or suspect data that occurred over a longer period, a "gap proportional filler" program was developed to fill these periods using a uniform and reasonable criterion. As the program name implies, the gaps (or periods with missing data) were filled using proportional relationships between that sensor when it provided "good" data and data from another sensor.

For each column (i) (i.e., raw data from an individual sensor with missing or suspect data), a reference column (j) (i.e., raw data from another sensor with reliable data over the time period) was chosen to be used later for the filling process. To find the most appropriate reference column for each sensor, this program first does a correlation analysis between all columns with data in the file. Then an indicator value is calculated between each pair of columns (i , j) by multiplying the r^2 value and a proportion between the number of valid data

that column j had when there was a missing value for column i, and the total number of data in the columns. Thereafter, the column with the maximum indicator value is selected as the reference column, which is then used to estimate the missing values (i.e., to "fill gaps").

Afterwards, the program scans data within columns until it finds a place with missing values. When a missing value is found, it calculates two mean proportions (one before and one after the gap) between the values in the column that has the gap and the corresponding values in the reference column. The number of timesteps before or after the gap used to calculate the mean proportions can be specified externally by the user in an options file (in this study we used 20 days before and after for the gaps smaller than 15 days, and 60 days for the gaps between 15 and 50 days).

Within a gap, an averaged proportion was used to fill in the missing values. This average was weighed between the proportions before and after depending on the position of the data to fill in within the gap. For example, if the gap had a length of nine missing values, the averaged proportion for the third place in the gap is going to be 1/3 of the proportion before the gap plus 2/3 of the proportion after the gap.

Several filtering conditions were established for the "gap filler"; in future uses of this program, these can be altered via an options file:

The length of the gaps to fill in could not be greater than 50 days

The values that were more than 2.5 standard errors apart of the mean were not taken in account to calculate the proportions between sensors.

The r^2 between sensors i - j had to be bigger than 0.7 in order to become i the reference sensor of j.

Program 5: Daily integrator

This program transforms the instantaneous sap flux density readings taken every 20 minutes into daily values. The trapezium rule was applied to calculate the area under the curve. The area of a trapezium was calculated per timestep and then summed for the whole day.

Scaling up sapflow density from individual sensors to stand level

Calculating sap flow at the stand level from the sensor level measurements, involved three steps. First the sensor measurements (sap flux density) were averaged to the individual tree level, then the tree measurements were averaged at the species level, and finally the species-level averages were scaled to the stand level by multiplying by the total sapwood area per hectare of each species in the stand. Special attention is given here to the first step.

Scaling up the sapflow density measurement to the tree level:

Granier-style sensors measure average velocity of the sap along the sensor in the particular place of the stem where the sensors are located. Therefore, to estimate the total flux at the tree level, calculations and assumptions must be made.

The first assumption is that the stem is a cylinder with an inner part (the heartwood) that is not conducting water, and an outer ring where the water transport occurs (the sapwood). Then one must account for the radial pattern of the flow within the sapwood, because the velocity of the water is typically different in the outer than in the inner part of the sapwood. Another assumption is that this radial profile of velocities is uniform within species at the same height above ground.

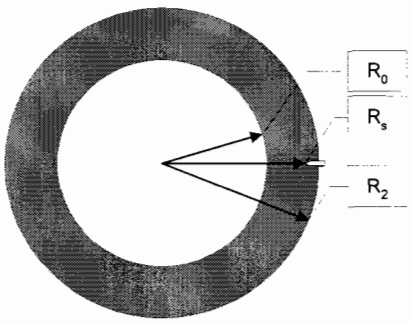

Fig 2.1 – Cross sectional representation of a stem with a sapflow sensor installed. R_0 : heartwood radius. Rs: sensor radius. R_2: sapwood radius.

In western hemlock, it was found that the sap velocity decreased linearly from the outer (i.e., next to the vascular cambium) to the inner sapwood, being zero at the boundary sapwood-heartwood (F. Meinzer, unpublished data; Moore et al. in press). Therefore, to calculate the average sap flux density within whole trees, accounting for the radial pattern, the following integration procedure was made:

Sap Velocity (v):

$$v(r) = r - R_0 \qquad (3)$$

Where r is a variable radius and R_0 is the heartwood radius.

Then sapflow ($\bar{J}$) can be calculated as the integration of the sap velocity over the sapwood area:

$$\bar{J} = \int_A v \, dA \qquad (4)$$

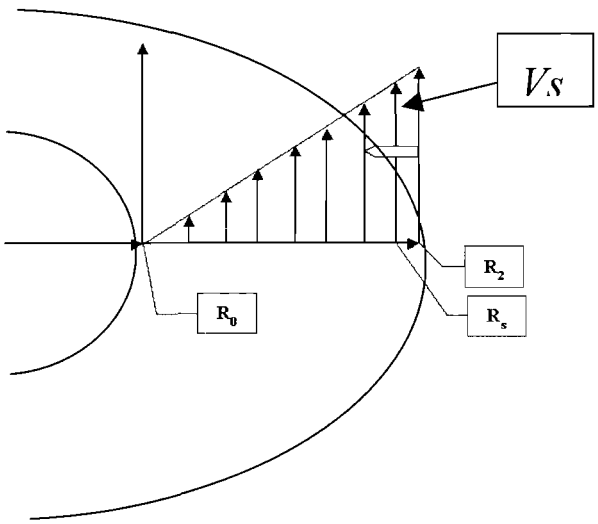

Fig 2.2 – Radial profile of sap velocities of a stem with a sapflow sensor installed. R_0 : heartwood radius. Rs: sensor radius. R_2: sapwood radius. Vs: mean sap velocity measured by the sensor.

Defining the sapwood area as the area between the sapwood radius (R_2) and the heartwood radius (R_0) then:

$$\bar{J} = \int_{R_0}^{R_2} \int_0^{2\pi} v(\theta, r) \; r \, d\theta \; dr \qquad (5)$$

Given the radius where the sensor was installed (R_S), and the measured sap velocity in that point (V_S):

$$\bar{J} = \int_{R_0}^{R_2} \int_0^{2\pi} \frac{r - R_0}{Rs - R_0} Vs \; r \, d\theta \; dr \qquad (6)$$

$$\bar{J} = \frac{Vs}{Rs - R_0} \int_{R_0}^{R_2} \int_{0}^{2\pi} (r - R_0)\ r\ d\theta\ dr \qquad (7)$$

$$\bar{J} = \frac{Vs}{Rs - R_0}\ 2\,\pi \int_{R_0}^{R_2} (r - R_0)\ r\ dr \qquad (8)$$

$$\bar{J} = 2\,\pi\ \frac{Vs}{Rs - R_0}\ \left[\ \frac{r^3}{3} - R_0\ \frac{r^2}{2}\ \right|_{R_0}^{R_2} \qquad (9)$$

$$\bar{J} = 2\,\pi\ \frac{Vs}{Rs - R_0}\ \left[\ \frac{R_2^{\,3}}{3} - R_0\ \frac{R_2^{\,2}}{2} - \frac{R_0^{\,3}}{3} + \frac{R_0^{\,3}}{2}\ \right] \qquad (10)$$

$$\bar{J} = 2\,\pi\ \frac{Vs}{Rs - R_0}\ \left[\ \frac{R_2^{\,3}}{3} - \frac{R_0\ R_2^{\,2}}{2} + \frac{R_0^{\,3}}{6}\ \right] \qquad (11)$$

To account for the radial pattern of sapflow in Douglas-fir, a relationship was used between inner and outer rings of sapwood, as described by Phillips et al. (2002). This relationship depends also on the diameter at breast height (DBH).

In this procedure, two mean sap velocities are calculated, one for the outer ring of sapwood (0-20mm inside the cambium) and the other for the inner ring (15-35mm inside the cambium). For the trees where the sapwood depth was greater than 35mm, it was assumed that the sap velocity was the same as the mean calculated for the inner ring. The relationship between the mean sap flux density of these two rings is described by the following equation:

$$\bar{J}_{in} = \bar{J}_{out} * 1.27(1 - e^{-2.44DBH(m)}) \qquad (12)$$

In our measurements of Douglas-fir, the sensors were measuring the outer sap flux. Therefore, to scale up the measurements to the tree level, the equation used to calculate the mean sap flux density per sapwood area was:

$$\bar{J} = \bar{J}_{out} * \frac{SA_{out}}{SA_{total}} + \bar{J}_{out} * 1.27(1 - e^{-2.44DBH(m)}) * \frac{SA_{inner}}{SA_{total}} \qquad (13)$$

Being:

SA_{out} = Sapwood area of the outer ring of sapwood.

SA_{inner} = Sapwood area of the inner ring of sapwood.

SA_{total} = Total sapwood area of the tree.

Soil Moisture

Soil volumetric water content was measured in six different sites (three old growth and three young) using dielectric probes (ECH2O dielectric aquameter model E-20, Decagon Devices, Inc.); from here on these will be called Echo probes. We dug one soil pit per site up to 2.2 meters deep, except in the "Young 2" site where we could not dig deeper than 1.4 meters due to coarse rocks. The pits had a rectangular shape on the surface, with approximate dimensions of 1m x 2.5 depending on the stability of the soil. On one of the ends, we dug a series of steps to allow us to enter the pit. The Echo probes were inserted on the vertical wall on the opposite side of the steps,. To avoid desiccation of the soil surrounding the probes due to evaporation from the open wall, the probes were installed such that the measuring part of the sensors was 35cm from the cut edge, and the vertical surface was then covered with a plastic tarp. To install the probes we removed a small amount of soil from the first 35cm with a core, and kept it to refill the hole after installing the sensors. After removing this soil, a steel blade of a similar size, but slightly thinner than the probes (which are thin rectangles, approximately 1rnm thick, 30rnm wide and 254mm long) was used to make an initial hole in the soil, and then the Echo probes were inserted into the space. In that way, the sensitive part of

Site	Depth				
Young 1	20cm	40cm	80cm	140cm	200cm
Young 2	20cm	40cm	80cm	105cm	
Young 3	20cm	40cm	80cm	140cm	200cm
Old Growth 1	20cm	40cm	80cm	140cm	
Old Growth 2	20cm	40cm	80cm	140cm	180cm
Old Growth 3	20cm	40cm	80cm	140cm	185cm

Table 2: Depth of the Echo probes per site

the probes was in tight contact with the surrounding soil. We installed six probes in each soil pit at the depths described in Table 2. At two sites, coarse rocks prevented installation of probes at the intended maximum depth of 2 meters; in two others, the water table was above that depth.

Calibration

Initially, I used the factory calibration formula (θ (m^3/m^3) = $0.000695mv$ - 0.29 , Decagon 2002) to transform the ECHO sensors' voltage output to soil volumetric water content(θ). The values turned out to be unreasonably low (i.e., θ (m^3/m^3)< 0). Therefore, I compared my measurements from the ECHO sensors with soil moisture measurements made with calibrated Sentek frequency domain capacitance sensors (Sentek PTY, Adelaide, Australia), that had been installed at the same sites over the same time period. Sentek sensors were installed as part of a project led by Drs. Renee Brooks and Rick Meinzer. This comparison confirmed that the ECHO measurements were consistently low. I performed multiple linear regression analyses to further explore the discrepancy between ECHO and Sentek measurements, and to determine whether I could use a simple equation to calibrate the ECHO probes for our soils.

Statistical Procedures:

Six Sentek probes had been installed at each site (old growth, young), and these were all within 20 meters of my ECHO probes at the young site, and 100m at the old growth site. The Sentek probes were configured to read and store data from eight depths at 15 min intervals continuously through time. For my analyses, I used measurements from specific depths that corresponded to depths measured with ECHO probes for a few discrete days, selected to represent a broad range in θ. For the old growth site, I used data from four days (205, 215, 235 and 255) for four depths (20, 40, 80 and 150cm). For the young site, I used data from five days (205, 215, 235, 255 and 261) for five depths (20, 40, 80, 150 and 200cm). I extracted data for three hours during the night (from 24:00 to 3:00) when the soil moisture content is most stable, and for each site I calculated the mean value for the six probes at each depth and over each time period. Similarly, I calculated the average measurement from the ECHO probes for the same depths and periods. Note, however, that at one of the depths, there was a slight offset between two measurement devices. The ECHO probes were installed to

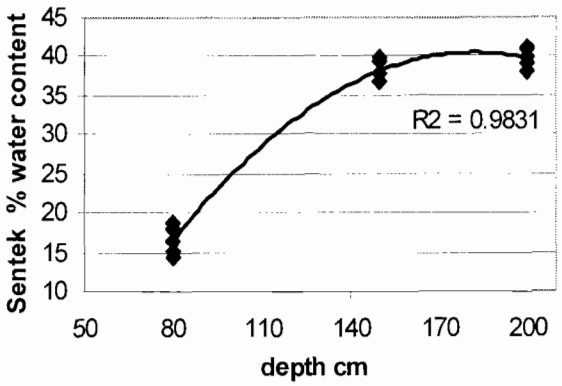

Fig. 2.3 – Soil water content calibration - Blue rhombus are water content (% volume) measurements with the Sentek equipment for data from five days (205, 215, 235, 255 and 261) for three depths (80, 150 and 200cm). Black line is adjusted quadratic regression, used to estimate water content at 140cm depth.

measure at 140cm, whereas the Sentek probes were configured to measure at 150 cm. I adjusted the Sentek data to account for this discrepancy as follows: A quadratic equation was fit to model Sentek measurements of θ for the 80, 150 and 200cm depths of the young site for the days mentioned above (fig. 2.3). Using this equation, an average proportional difference between the 150cm depth and the 140cm modeled water content was calculated. Afterwards the Sentek soil moisture data from150cm depth at the old growth site was transformed to estimate soil moisture content at 140cm depth using that proportional difference (0.0436).

Several multiple regression models were tested to select the most suitable equation to model the relationship between the ECHO and Sentek sensors. The models ranged from a simple linear regression with the ECHO data as the independent variable ($\theta_{Sentek} = a*\theta_{ECHO} + b$) to a multiple linear regression including indicator variables for each depth and site ($\theta_{Sentek} = a\ \theta_{ECHO} + b *\theta_{ECHO} *$ isY1 + $c*\theta_{ECHO} *$ is40 + $d*\theta_{ECHO} *$ is80 + $e*\theta_{ECHO} *$ is140 + $f*\theta_{ECHO} *$ is200 +g). One objective of this analysis was to test whether a simple model could be applied to data for both sites and all depth, or if different equations should be used for different sites or depths.

The simple linear equation provided a good explanation of the relationship between θ_{ECHO} and θ_{Sentek} ($r^2 = 0.882$, p-value< 0.001). The best model based on Bayesian Information Criterion (BIC), Akaike Information Criterion (AIC) and

extra sum of squares F-test values (Ramsey & Schafer, 1997) included an indicator variable for the 140cm depth. However, for the sake of simplicity, I decided to use the simple linear regression equation to model the relationship between the two sensors. Although the additional variable in the more complex model is statistically significant (difference in r^2= 0.05), the improvement on the prediction of θ_{Sentek} is small relative to the intrinsic measurement errors of the instruments and variability within the sites. Consequently, I selected the simple linear model: $\theta_{Sentek} = 1.0882 * \theta_{ECHO} + 12.68$. With a 95% confidence interval the slope of this linear equation was not statistically different from 1, (CI 95% = 0.959, 1.217). Therefore, I decided to use a simple scalar (the intercept of the equation) to "correct" θ_{ECHO} measurements. This procedure, of course, requires the assumption that the Sentek measurements are "true". Ongoing tests in our laboratory are further refining the calibration process, but for the purpose of this thesis, I had no other recourse than to rely on the Sentek data.

The r^2 of predicted vs. observed relationships (where "predicted" are the corrected values for θ_{ECHO} measurements, and "observed" are θ_{Sentek} measurements) are the same whether a slope is used in addition to the intercept, or only the intercept. All of the subsequent soil moisture measurements in this thesis are data from the ECHO probes, corrected by an offset of 12.68 (CI 95%=10.69 , 14.67)

Root Biomass

To parameterize the SPA model, root biomass data were used that were collected by Dr. Kate George at the same study sites. Soil cores were removed from the six soil pits (see details above) at 20 cm depth intervals to a depth of 120cm. Samples were taken from all six sites (three young and three old-growth). Five samples from an area comprising $1m^2$ per site were cored for replication. Roots were removed by hand in the laboratory from each core and sorted into four size classes (<1mm, 1-2mm, >2-5mm, >5mm). Then roots were dried and weighed. Standing root biomass (g m^{-2}) was calculated for each depth interval based on the area of soil core (40.72 cm^2).

Photosynthetic capacity

The SPA model requires measurements of photosynthetic capacity. I used data measured by Dr. Julia Kerrigan at the same three young and three old-growth sites used in my studies

Douglas-fir branches exposed to full sun were collected from 5 trees per site, in May – June 2002. Collections from the young sites were done by myself; I used a shotgun in two of the sites and hand clippers in the third, where a tower provided access to upper-canopy branches. In the old growth sites, the collections were performed by professional tree climbers. Measurements were made on one-year-old needles.

A/Ci curves (measured by Dr. Julia Kerrigan)

A/Ci response curves (net CO_2 assimilation rate (A) versus calculated internal CO_2 concentrations (Ci)) were measured using a LiCor 6400 portable photosynthesis system (LiCor, Inc.). Cuvette conditions were maintained at PPFD = 1600 mmol m^{-2} s^{-1}, temperature = 20 °C, and air flow rate = 100 mmol m^{-2} s^{-1}. Ambient CO_2 concentration (Ca) in the cuvette was controlled with a CO_2 mixer across the series of 40, 30, 20, 40, 60, 80, 100, 120, 160, and 200 Pa, and measurements were recorded after CO_2 assimilation equilibrated to a steady state (CV < 2%). The projected area of foliage in the cuvette was quantified digitally using a video image recorder and AgVision software (Decagon Devices, Pullman WA). Non-linear regression techniques, based on the equations of Farquhar et al. (1980) and later modified by Sharkey (1985) and Harley and Sharkey (1991), were used to estimate Vcmax (rubisco activation rate), Jmax (light saturated rate of carboxylation limited by electron transport), and R_{day} (rate of respiration in the presence of light) for each A/Ci curve. As discussed elsewhere (e.g., Harley et al., 1992; Wullschleger, 1993), it is necessary to first designate an internal CO_2 concentration threshold at which the A/Ci curve switches between the rubisco- and electron transport-limited portions of the curve. By selecting Ci values below some threshold, it is assumed that A is limited by the amount, activity, and kinetic properties of rubisco (Wc), and the remaining portion of the A/Ci curve is used to solve for the Wj curve and Jmax. Vcmax, Jmax, and R_{day} were calculated for each A/Ci

curve by designating 40 Pa as the cut-off value, and adjustments were made if necessary (i.e., if, based on the slope, a lower or higher cut-off value appeared to provide a more appropriate estimate). The carboxylation rate at Ca = 40 Pa ($Wc_{\_ACI}$) was calculated from equation 14:

$$W_{c\_ACI} = \frac{V_{c\max} \cdot C_i}{C_i + K_c(1 + O/K_o)} \qquad (14)$$

where: Kc and Ko are the Michaelis-Menten coefficients for CO_2 and O_2 binding to rubisco, and O is the intercellular partial pressure of O_2 (21 kPa).

The averaged Vcmax , Jmax and R_{day} for the old growth and the young trees were used as inputs of the model. Due to lack of similar data for other species, the values for Douglas-fir were assumed to be representative of all species at each site. This assumption is not likely to cause a large error at young sites because Douglas-fir accounts for a very large proportion of total leaf area, but it could lead to errors at the older site. If anything, the assumption probably leads to an overestimate of carbon assimilation at the old site, since photosynthetic capacity of Douglas-fir (even old growth) is greater than that of the shade-tolerant conifers at the site (Bond et al. 1999; Thomas and Winner 2002).

Throughfall and Canopy Storage of Rainfall

(The measurements and data collection of these variables were done by Tom Pypker.)

Rainfall events can be partitioned into two separate phases: pre and post canopy saturation. Prior to saturation the rainfall reaching the forest floor is primarily comprised of droplets that fall directly to the forest floor. The cumulative net precipitation (P_n) prior to canopy saturation will proceed a rate less than the gross precipitation (P_G) (i.e., $P_n<P_G$, where the P_n/P_G for any point prior to canopy saturation <1 and equal to p). Once the canopy saturates ($P_G=P_S$, where P_S is the canopy saturation point), P_n will track P_G more closely (Fig.1), where P_n is always less than or equal to P_G. If P_n is less than P_G, then the difference between the two is the evaporation during the storm (E).

The method used to calculate the rainfall variables is outlined in Link (2001). In brief, the canopy parameters of canopy storage (S), throughfall (p), E, and interception loss (In) were calculated by using the relationship between P_n and P_G (Fig. 2.4). Prior to canopy saturation the relationship between them is calculated as:

$$P_n = pP_G \qquad (15)$$

Where *p* is the proportion of rainfall that passes through the canopy prior to canopy saturation. Subsequent to saturation, the rainfall either drips to the

forest floor or evaporates back to the atmosphere. Hence, following saturation the rainfall beneath the canopy is then described as:

$$P_n = pP_S + (1 - \frac{E}{R})(P_G - P_S) \quad (16)$$

where: E/R is the ratio of evaporation to rainfall during canopy saturation and $P_n \leq P_G$. The variables of p, E/R and P_S are estimated by minimizing the sum of squares for regression equations 15 and 16. S is then computed by finding the inflection point between the two equations and removing the rainfall lost to evaporation during canopy wet-up (Equation 17):

$$S = (1 - p)P_S - I_W \quad (17)$$

Where I_W is the rainfall that is evaporated during canopy wet-up. I_W was estimated by:

$$I_W = (E / R)P_S \quad (18)$$

Here E is considered constant throughout the storm.

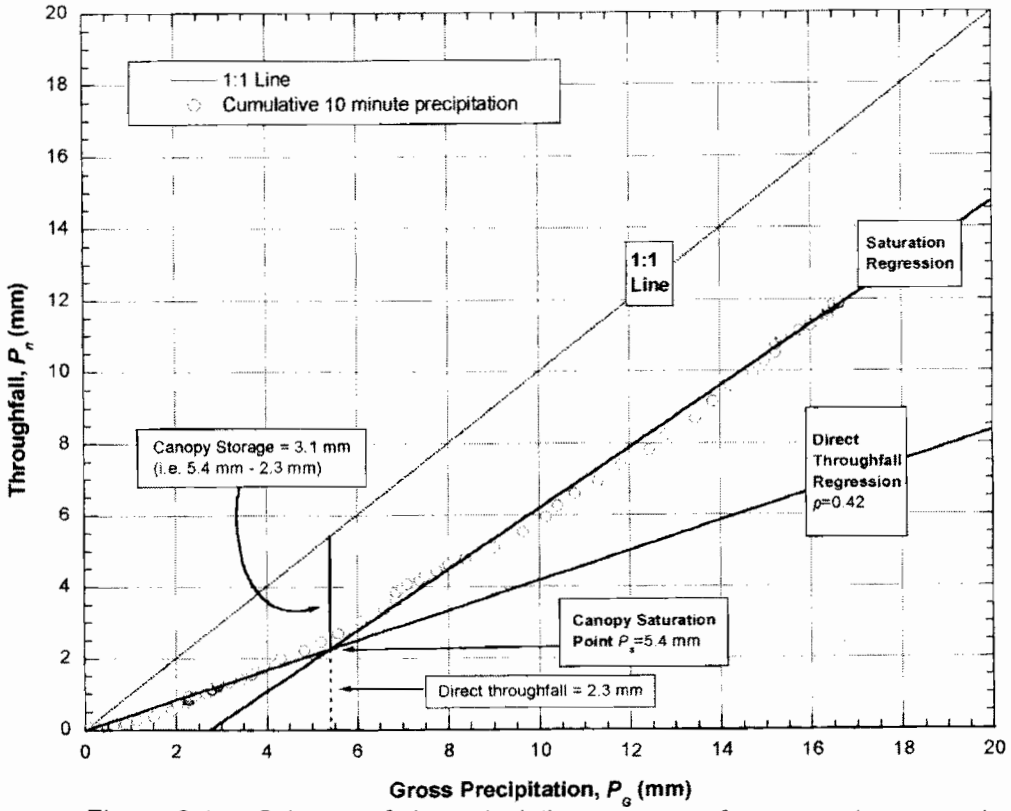

Figure 2.4 – Scheme of the calculation process of canopy storage and direct throughfall. From: Tom Pypker, unpublished data

Throughfall measurement

Throughfall was measured using a roving array of 24 tipping bucket rain gauges (TE-525I, Texas Electronics Inc., Dallas, TX, USA) from 1 June to 30 November 2002. Each tipping bucket rain gauge has a collection area of 325 cm^2, has a resolution of 0.254 mm, was placed 1 m above the ground and the data were stored on individual micro-dataloggers (HOBO event, Onset Computer Corp., Pocasset, MA, USA). Two roughly perpendicular 70 m transects were established and each transect had half of the tipping bucket array placed randomly along it. The tipping bucket array was complemented by a second array of 48 manual throughfall collectors. The manual throughfall collectors had

a 94 cm^2 collection surface and were used to verify the estimates provided by the tipping bucket array (15 September to 30 November, 2002). The tipping bucket array and the manual throughfall collectors were randomly relocated every 4-6 weeks to reduce sampling errors. The gauge funnels and tipping buckets were cleaned and leveled every 4 weeks.

Phenology

The phenological data were collected for the year 2002 by Tom Pypker and Dr. Barbara Bond for the six sites (three young and three old growth). After a visual examination, a numeric code was assigned to represent the phenological stage of the majority of vegetation present. Codes were as follows:

Phenology coding scheme:

0=no swell

1=swell

2=showing green tips but no leaf expansion

3=buds broken, leaves showing but little or no stem elongation

4= stems elongating

5= stems fully expanded

Phenological assessments were performed weekly starting on May 9th, until the majority of the plants reached phase 5.

Description of the original SPA model

(adapted from Williams et al. 1996, and Williams et al.2001)

The model consists of various sub-models, which can be roughly divided into physical and biological components. The physical cornponents specify the structure of the canopy, determine the absorption of both photosynthetically active radiation (PAR) and other wavelengths in each canopy layer, calculate leaf boundary layer conductance, and determine soil water availability. The biological components determine how leaf water potential varies with transpiration, the variation of leaf biochemical parameters with foliar N content, irradiance and leaf temperature, and the diurnal course of stomata conductance in each layer, which controls C uptake and water loss.

Physical sub-models

The physical sub-models are calculated only once per time step (30 min). Half-hourly meteorological data were needed to estimate micrometeorological conditions within the stands. There are four physical sub-models.

(A) Canopy structure

The canopy is divided into 10 layers, spaced uniformly. The leaf area per layer is specified in an input file according to the leaf area vertical distribution of the stand. The variation in N concentration (g m^{-2} leaf area) is also specified in an

input file or it is calculated with an exponential decay function that describes its vertical distribution.

(B) Radiation regime

The radiation routines simulate the incidence, interception, absorption, and reflection of PAR, near infrared radiation (NIR), and long-wave radiation. The diffuse fraction of the incoming flux is estimated from the integrated daily total PPFD (μmol $m^{-2}s^{-1}$). The incidence of NIR (i.e., the remaining component of the short-wave radiation) is approximated using relationships from Szeicz (1974).

To determine solar radiation absorption, Beer's Law is used as described in Amthor (1994). Their multi-layer model of radiation absorption by the canopy accounts for individual leaf and forest floor reflectance and absorptance of NIR, PAR and long-wave radiation. A spherical leaf angle distribution is assumed. The sum of PAR (derived from PPFD), NIR and long-wave radiation absorbed determines the net isothermal radiation for each canopy layer.

(C) Leaf boundary layer characteristics

The multi-layer approach requires to estimate the variation of boundary layer characteristics of leaves within the canopy. This is based on the wind profile in the canopy. However, wind speeds, and thus boundary layer conductance, decline in the canopy (Roberts et al.1990). For each canopy layer, the leaf

boundary layer conductance to water vapor and heat is estimated using relationships from Nobel (1983).

(D) Soil water characteristics

Soil water potential (ψ_s) and soil hydraulic conductivity (L_{soil}) were not measured directly for the original model application, but estimated from soil sand, clay and water content using empirical relationships (Saxton et al.1986). Evaporation of water from the soil surface is determined from soil radiation balance and soil water content (Amthor et al.1994).

Biological sub-models

The key hypothesis governing the biological components of the model is that stomatal conductance (g_s), is controlled to maximize carbon gain per unit N within the limits set by the rate of water uptake and canopy water storage. Meinzer and Grantz (1991) hypothesize that g_s, will ideally remain in balance with the hydraulic capacity of the soil and roots to supply the leaves with water, avoiding leaf desiccation at one extreme and the unnecessary restriction of CO_2 uptake at the other. This is modeled explicitly; the impact of stored water, or capacitance, is also included. Plants are assumed to open their stomata until either (1) further opening does not constitute an effective use of stored water in

terms of carbon gain per unit water loss, or (2) further opening causes a drop in leaf water potential below the limit that causes xylem cavitation.

Plant water relations are modeled as an analogue to a simple electrical circuit. Each canopy layer is assumed to have an independent connection to soil water. Therefore, each layer is modeled separately.

Roots-Soil resistance

The original model used a sub-model of steady-state conditions of a single soil layer to estimate the hydraulic resistance of the soil around the roots that supply each canopy layer. The single soil layer was not an appropriate approximation for this study because of the seasonal drought of the area, and the approach done by Law et al. (2000) was adopted for this study. The model is dependent on root dimensions and soil hydraulic conductivity. It is assumed that an equal proportion of the total root length supplies each canopy layer, and so the root resistance related per canopy layer is invariant among canopy layers. However, as soils change the water content hydraulic conductance per soil layer changes consequently.

Plant hydraulics

The highest layers in the canopy are subject to the greatest resistance to xylem water supply. Thus, xylem hydraulic resistance per unit leaf area for layer n in the canopy increases with the layer height (h). Various simplifying assumptions

are done in the representation of plant hydraulics. Analogous with a pipe model, each layer is served by an independent water supply system. The model employs an unbranched rather than a branched scheme, because of its greater simplicity and because it represents a canopy of many individuals, rather than a single tree.

The water in the xylem can cavitate under the extreme tensions that occur naturally, and there is often a threshold water potential for such cavitation (Jones 1992). The onset of xylem cavitation can lead to a rapid and catastrophic decline in stem hydraulic conductivity by inducing further cavitations (Tyree and Sperry 1989). Jones and Sutherland (1991) have shown that the maintenance of a maximally efficient conducting system requires that stomata close as evaporative demand rises to prevent shoot water potentials falling below this species-specific threshold value (ψ_{lmin}).

Dynamic flow

The relationship between the water flux through the plant and the water potential drop is not unique; initially water is drawn from stores in plant tissues, so that liquid flow lags the transpirative demand (Landsberg et al.1976; Schulze et al. 1985). This hysteresis can be simulated by incorporating capacitors into the circuit analogue to represent canopy water storage capacity (Jones 1978).

Leaf biochemical parameters

Algorithms used to model photosynthesis are based on kinetics described in Farquhar and Von Caemmerer 1982. Photosynthesis is limited by the minimum of the ribulose bisphosphate carboxylation rate and the rate of ribulose bisphosphate (RUBP) regeneration. The maximum rates of these two processes were calculated by Dr. Julia Kerrigan. These photosynthetic parameters are proportional to the foliar nitrogen content of each canopy layer.

Impacts of water status

It is assumed that the photosynthetic apparatus is resistant to drought. Therefore, it is also assumed that water stress affects only g_s and not the photosynthetic mechanism.

Leaf level processes

For each canopy layer, an iterative procedure is performed at each timestep to determine the maximum stomatal conductance in each layer (g_{sn}) and the assimilation rate associated with this conductance.

The iterative process is as follows, starting from a very low g_{sn}:

1. Increment g_{sn} by a small amount (c. 1 mmol m^{-2} s^{-1}).

2. Determine leaf temperature (T_l, °C) resulting from the leaf energy balance at this g_{sn} using a steady-state approximation (Jones 1992).

3. Determine leaf biochemical parameters, based on foliar N concentrations (Field and Mooney 1986), absorbed PPFD and leaf temperature.

4. Determine the equilibrium mesophyll $C0_2$ concentration (C_c) that satisfies both diffusion from the atmosphere to the mesophyll and metabolic uptake, as described by Farquhar and Von Caemmerer (1982).

5. Calculate transpiration rate (mmol m^{-2} s^{-1}) for this canopy layer at this g_{sn}, with the Penman-Monteith equation (Jones 1992).

6. Calculate the change in layer leaf water potential (ψ_{ln}) after one time step (Δt, 1800 s) of transpiration at the specified g_{sn}.

7. Return to step 1 (for a further increment of g_{sn}), unless either:

    i. Previous g_{sn} increment failed to raise assimilation appreciably (see below), or :

    ii. ψ_{ln} has reached its specified limit (ψ_{lmin}). The water supply system is now operating at its maximum rate; any further increase in g_{sn} would take the xylem beyond its threshold for cavitation, potentially resulting in a catastrophic failure in water supply.

This iterative proces of setting g_{sn} especially as it relates to step (7), sets the canopy model apart from similar models. Embedded in this procedure is the underlying hypothesis that stomata operate to minimize water stress, by effectively using stored water to maximize C gained per unit water loss over the course of the day, and by preventing xylem cavitation.

Model Scheme

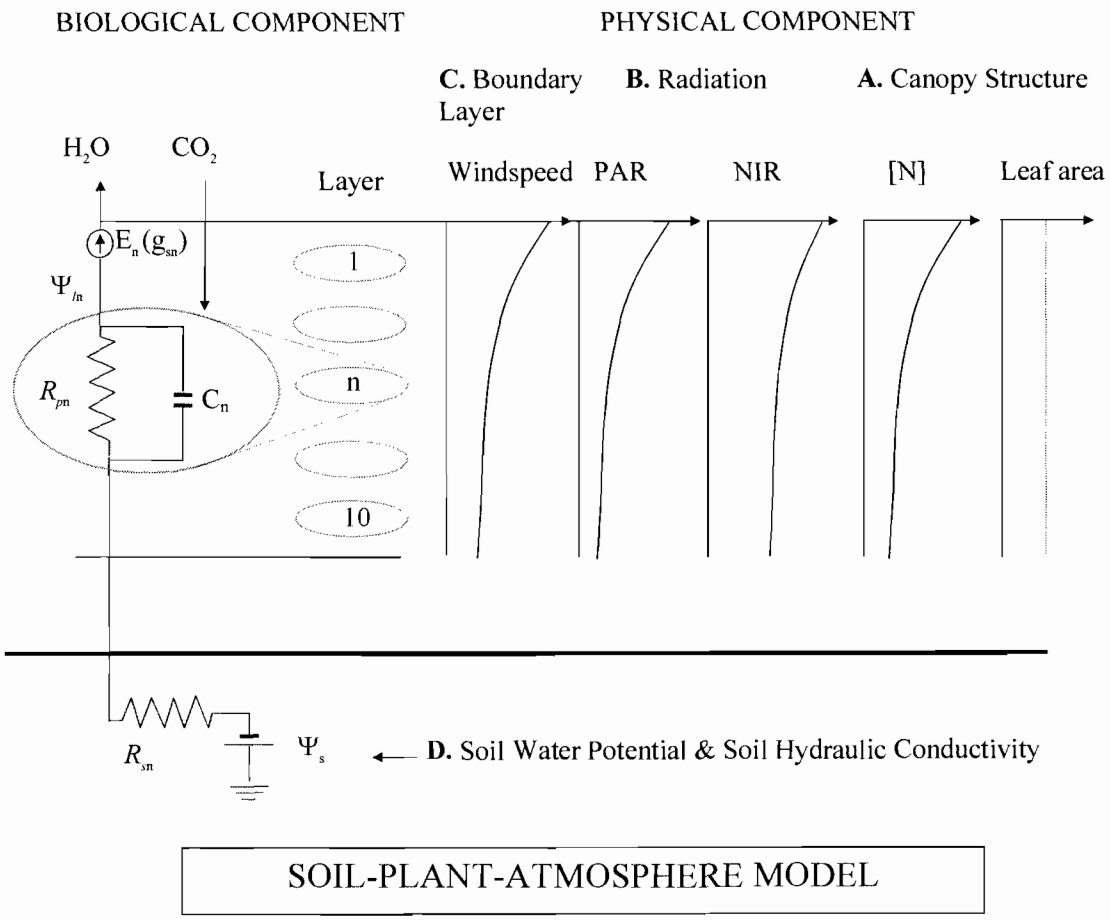

Figure 2.5 - The canopy model is divided into physical and biological components. The former have four facets, consecutively calculated as lettered in the diagram, relating to (A) the variation in leaf area index (LAI) and leaf nitrogen content ([N]) with depth in canopy; (B) the vertical distribution of radiation - PAR, NIR and long wave (not shown); (C) the distribution of wind speed and boundary layer conductance within the canopy; and (D) the soil water potential (ψ_s) and soil hydraulic conductivity. The biological component is then applied successively to each canopy layer. Biological processes are calculated iteratively by incrementing stomatal conductance (g_s) until this results in either no significant increase in A (i.e., A is limited by light or metabolic rates), or the minimum leaf water potential (ψ_{lmin}) has been reached.

From: Dr. Mathew Williams, scheme of SPA model first version, personal communication.

Features added to the model for this study

Many changes were made to the code of the program in order to increase the functionality of the program and make it more "user friendly". The following sections summarize the modifications made.

Changes to Input / Output management

In the original program, it was impossible to run without having knowledge of Fortran language and a Fortran 90/95 compiler to create the executable file after specifying at least the location and names of the input files. To completely parameterize the model, it was necessary to change values imbedded in the code of the program and then recompile. Therefore, I modified the program so that these values or settings can be specified in external files. In this way, anyone can use the program and do a complete parameterization of the model to different sites using an executable file for the program, without having to modify the Fortran code.

Setting the file names and location

In the original version of the program, the location and name of the input files needed to run the program had to be specified in the source code of the program. In the new version of the program, all the input files needed to run the program and the location for the output files are specified in an external text file.

The only condition needed to be able to run the program is that the "settings.txt" file has to be located in the same directory as the executable file.

New Options file

To increase the functionality of the program some new features were added and users may specify whether they want to use these features or not. Some of these modifications were added to increase the efficiency during the fitting process (i.e., comparing model output to measured data during the parameterization process), where only some of the features of the model are needed. In order to reduce the time consumed to complete a run and/or reduce the memory needed to allocate the output files, the user can select to run the program having "on" only the features required for that purpose. Consequently a comma delimited values file was created to let the user of the program choose which of these options wants to use:

- Read water content from an external file or make the model calculate it.
- Perform a sensitivity analysis on one variable at a time or with all possible combinations of variables.
- Generate output files for each canopy layer or only general ones for the stand level
- Select the range of Julian days to run the model.

- Select the range of Julian days to write in the detailed output files (30 minutes timestep).

- Check the goodness of fit against 30 minutes sap flux data or not.

- Check the goodness of fit against daily sap flux data or not.

- Specified the weights for the goodness of fit Indicator described in MacKay et al. 2003.

- Decide whether to print or not, any of the following cumulative variables, for each iteration of the sensitivity analysis:

  GPP, NEE, leaf respiration, latent energy, sapflow, precipitation, runoff, discharge, transpiration, soil evaporation, and evaporation from wet surfaces

Variables assignments taken out of the code

To be able to apply the model to other ecosystems without having to deal with the Fortran code, it is necessary that the variables that have to be changed are reachable outside the program code. Therefore, all the variables that were adjusted during the parameterization of this study now can be assigned different values in an external file. The variables that were assigned a value inside the code and are now externally assigned: Vcmax, Jmax, maximum height, minimum height of the foliage, rain retention, maximum canopy storage, throughfall, live roots proportion, clumping.

Selection of the output files

In the previous version of the model, the program created all the output files for every run. The output files were generated in the same directory, unless specified in the code. This had the advantage that the memory required to store the output files was fixed, but the disadvantage that the output files were overwritten every run. Thus, if one wanted to keep a specific output file, one had to move it to a different folder or change the name of the file before running the program again. Consequently, it was very hard to handle consecutive runs of the model. In addition, the program was wasting CPU time writing files that were not used. Therefore, for all the output files a printing condition variable was added, and an external file was created to let the user select which output file he or she wants to generate when running the model program. Moreover, the program was modified in order to create a different folder per run where all the output files are going to be located.

Changes to Model Structure

Water content

Soil water content is calculated for each timestep by the model based on the use of water by the vegetation, evaporation from the soil surface, precipitation, and water movement between soil layers and possible vertical drainage out

form the system. To increase the versatility of the model, I added the option of allowing soil water content of the different soil layers to be provided as an input file. This is an important feature when trying to apply the model to stands where there is a significant lateral water movement. As the SPA model does not handle lateral movements of water, the way to avoid a misrepresentation of the soil water content is to make the program read in a daily basis the water content from an input file.

Changes to Phenology

To represent the seasonal change of the leaf area, a new input file representing the phenological development of the stand is required. This file should have the percentage of the total leaf area present per day. In this study, I transformed the phenological qualitative code files to quantitative ones. The assumption made were:

- There is a 25% leaf turnover per year.
- The increase in leaf area started when the stand was at the phenological code 2 (page 42-43) and finished when the stand was at code 5.
- The increase in leaf area was linear in time from code 2 to code 5.
- The decrease in leaf area started in day 275 and decreased at the same rate as the increase in the spring

Changes to rain infiltration

When exploring the soil moisture data measured at the sites, we noticed that when there was a rain event, the water penetrated rapidly into multiple soil layers (see figure 2.6). This rapid penetration of rainfall into the soil profile was found in several studies in forest and agricultural systems (Mosley 1979, McDonnell 1990, Knechtenhofer et al. 2003). The preferential flow pathways for rainfall could be originated by macropores present in the soil structure, vertical cracks, or lived and dead root channels. In contrast, the original model added the precipitation input to the upper soil layer and allowed the water to drain down according to the permeability of the soil when the water field capacity was reached for each layer. I changed the infiltration subroutine of the model in order to represent better the reality that the field data were showing.

The new subroutine allows adding the precipitation to multiple layers at the same time. A new variable (rain_retention) was created to permit a calibration of this feature to other situations, or return to the original subroutine if the value given to the new variable is equal to 1. In the revised model, the water reaching the soil at each

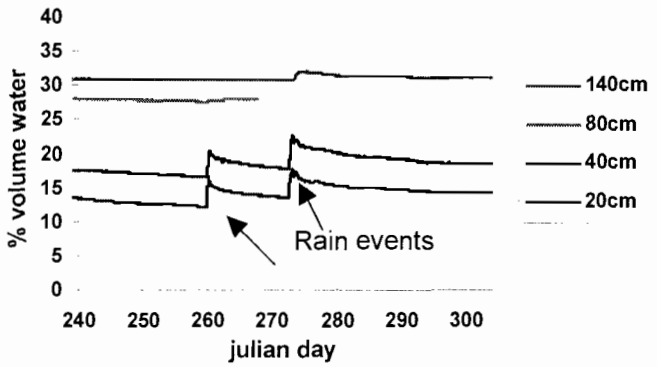

Figure 2.6 – Soil water content for the "rain retention" parameter calibration of the old-growth site.

timestep is multiplied by the rain_retention variable, which ranges from 0 to 1; this determines the amount of water that may be added to the first layer if it is not saturated. The remaining water is distributed among the deeper layers repeating the same procedure until there is no remaining water.

In this study, the rain_retention parameter was calibrated against the field measurements before and after the only two rain events recorded the summer of 2002 (fig.2.6; days 259 and 272) for the multiple depths measured. The rain_retention value that generated the best adjustment was 30%.

Changes to Facilitate Testing Goodness of Fit between Modeled and Measured Data

In the original version of the model, comparisons between the model output and field data had to be done externally, using other software. I added a new subroutine to the program to facilitate this comparison and make the calibration process faster. This subroutine compares the modeled sap flux data against measured sap flux data and calculates Pearson's r^2, the slope and intercept of the least mean squared errors regression line, the root mean squared error (RMSE), and an Index combining the first three parameters as described by Mackay (2003).

Sensitivity analysis algorithm

To increase the efficiency of the model, changes were made to allow automatic consecutive runs using incremented values of key parameters to evaluate the model sensitivity to these variables. To make this possible the software structure had to be changed while taking care that the logical structures of the SPA model calculations within a run were not changed. The input/output management modifications, explained above, were one aspect of this process.

In the previous version of the model, information was read and written to external files at each timestep. In the revised version, to decrease the average time required per run of the model, all the input files are read during the first steps of the program. New variable arrays were created to hold in the stack memory of the computer all the information needed to run the program. Then, the input files are rearranged in order to have all the scalar variables in the same input file. In that file, the user can choose the variables to vary in a sensitivity analysis by specifying the range of values and the interval of fluctuation for each variable. A maximum of five variables at a time is imposed. In this input file, the user can also select the root name of the folder where all the output files and folders are going to be located.

As mentioned before, the user can also select which of two types of sensitivity analysis to perform. One is varying one parameter at a time, and the other is

performing all possible combinations among the ranges and intervals specified for all the variables.

For each run of the model the goodness of fit against measured sapflow data can be performed. Therefore, a "fitting.csv" file is created to print the critical information that the user chose in the "options file.csv" together with the current values of the variables on which the sensitivity analysis is being done.

For each change on any of the variables, a new directory is created inside the main directory, with the root name specified by the user. The order of the subsequent folders depends on the type of sensitivity analysis performed, having a nested organization when the analysis is being done for all possible combinations.

Parameterization of the model

Total Leaf Area Index (LAI)

Leaf area index of the old growth stand (OG1) was extracted from Thomas and Winner (2000). They used an

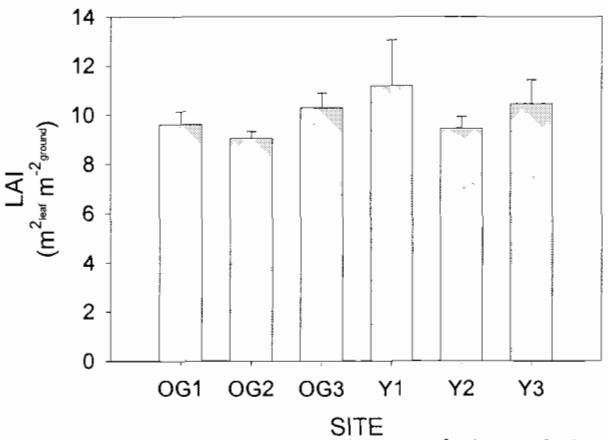

Figure 2.7- Leaf area index of 3 young and 3 old-growth sites.
From: Tom Pypker, unpublished data

adapted line-intercept technique, making direct measurements on the canopy of the old-growth site used in my study. Their value has been adopted as the most accurate estimate for the old-growth site, and has been referenced by many researchers (Parker et al. 2002, Bond and Franklin 2002, Chen et al. 2002, Fessenden and Ehleringer 2002). In addition, Tom Pypker used the LAI 2000 to estimate total LAI for all six sites used in this study during the summer of 2002. He found no significant differences between the LAI values for the six sites (fig. 2.7). Since the absolute value of the technique adopted by Pypker is less accurate than the direct measurements made by Thomas and Winner, I decided to use the LAI value estimated by Thomas and Winner for all of the sites.

Leaf Area distribution

The SPA model uses 10 canopy layers, and an estimate of the leaf area per canopy layer is needed. To parameterize the vertical distribution of leaf area for the model I used information from Parker et al. (2002). They estimated the leaf area variation at different heights in OG1 and Young1, using an inverted mean transmittance profile in accordance to Beer-Lambert rule, as described in Parker et al. (1997).

Parker et al. (2002) estimated the distribution of leaf area every one meter in the young site and every two meters in the old growth site. For the model, these detailed data were transformed from absolute amounts to fractions of the total leaf area, and distributed into 10 layers equally distributed in height as shown in figure 2.8. The canopy layers needed to be equally distributed in height in order to perform a sensitivity analysis of the impact of the maximum height on modeled physiological variables. The sensitivity analysis is described in more detail later, but I note here that when maximum height is varied, the proportional distribution of leaf area was maintained. (This was deemed important because the old and young stands have very different vertical distributions of leaf area) Therefore, to avoid an unintentional change in the leaf

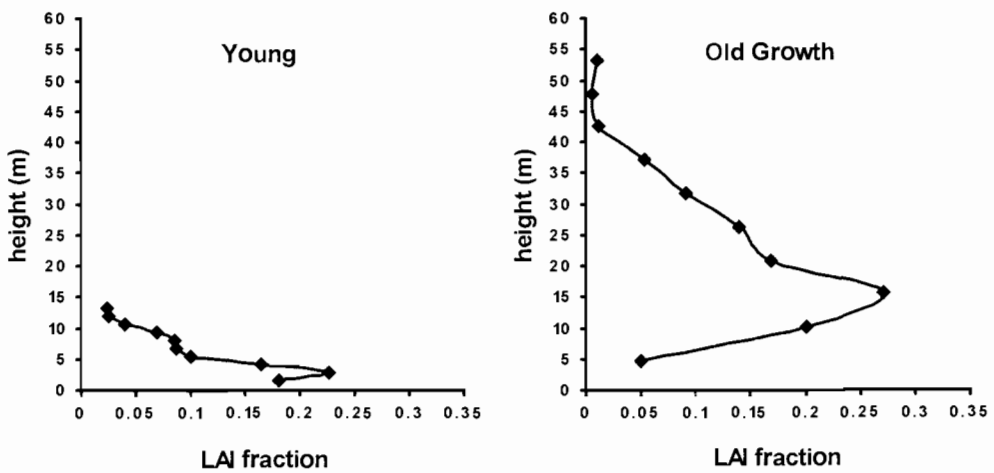

Figure 2.8 – Leaf area vertical distribution for both young and old-growth stands. Estimated using an inverted mean transmittance profile in accordance to Beer-Lambert rule, as described in Parker et al. (1997).
Adapted from: Parker et al. (2002).

area distribution when height was varied for the sensitivity analyses, the canopy layers had to be equally distributed with height.

Minimum Leaf Water Potential

The biological component of the model determines how leaf water potential varies with transpiration; stomatal conductance then regulates transpiration in order to maintain leaf water potential above a minimum threshold. A threshold value must be provided as input to the model. Estimates for this parameter were taken from McDowell et al. 2002b, who reported lower mid-day minima in the old growth stand (OG1; -2.6 MPa) than in the young stand (Young 1; -2.1 MPa). The values for the younger trees were consistent with the results published by Bond and Kavanagh (1999), for the same species. McDowell et al. 2000b speculated that the lower mid-day minimum water potential in the older trees might serve as a type of "compensation" for their greater hydraulic resistance, since the lower leaf water potential would result in a greater soil-to-leaf water potential gradient, which in turn should permit higher stomatal conductance averaged over time. One of the sensitivity analyses performed in the modeling study was designed to examine the impact of the lower leaf water potential on transpiration and carbon assimilation in the old stand.

Nitrogen fraction

To represent the changes in the photosynthetic capacity among canopy layers, the nitrogen concentration (on a leaf area basis) of each layer must be specified as an input variable. The highest nitrogen concentration, as well as the greatest photosynthetic capacity, occurs at the top of the canopy in the full sun leaves (e.g., Bond et al. 1999). As leaves are more shaded, less nitrogen is allocated to the leaves. In the SPA model, the maximum carboxylation capacity and the maximum electron transport rate are reduced proportionally with the reduction in foliar nitrogen, following Harley et al.1992.

To estimate the profile of foliar nitrogen on a leaf area basis, I used an equation described by Bond et al. (1999) that relates foliar nitrogen with the fraction of photosynthetically active radiation (FPAR) as a fraction of full sun.

$$N_{area}(g\ m^{-2}) = 1.26 + 0.353 * \ln(FPAR(\%))$$

Where N_{area} is nitrogen concentration per leaf area.

To obtain the FPAR value the radiation subroutines of the SPA model were used, using the information of the leaf area canopy profiles, a spherical leaf angle distribution, and a clumping factor of 1.

Sand and clay percent

Soil water potential (ψ_s) and soil hydraulic conductivity (L_{soil}) are important parameters in SPA for calculations of water flux. In the typical application of the model, these variables are estimated, from the fractions of sand and clay, which are provided as input variables, along with soil water content, which is updated during each timestep, using empirical relationships (Saxton et al.1986). However, the soils of the sites used in this study contain a large proportion of tephra, a volcanic porous material, and in this case the Saxton equations are not adequate to calculate and L_{soil} from sand, clay and water composition. Therefore, I employed a "backwards" approach to parameterize the sand and clay contents for the soils at Wind River. Using field measurements of ψ_s , and soil water content (θ), the Saxton equations were employed to empirically derive "effective" sand and clay percentage values for the upper 20-30 cm. The ψ_s

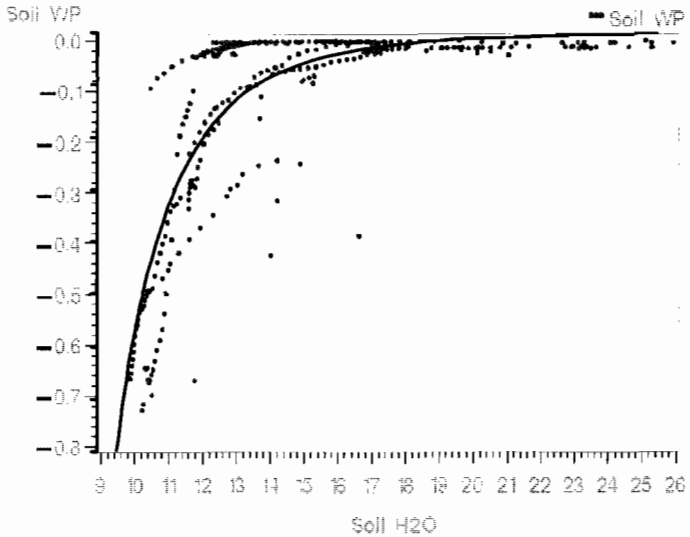

Figure 2.9 – Soil water release curve calibration. Soil water content (Soil H2O; % volume) versus soil water potential (Soil WP; MPa). Red points are measured data from Drs. J. Warren, F. Meinzer and R. Brooks. Solid line represents an adjusted curve through variations in sand and clay percent used on the empirical equations derived by Saxton et al. (1986) relating water content with water potential and conductivity.

and θ data came from measurements by Dr. Jeff Warren, who used soil psychrometers (PSY-55,Wescor, Logan, UT) to measure soil water potential, and the Sentek device (described above) to measure soil water content as part of a project led by Drs. Rick Meinzer and Renee Brooks. Their data for the OG1 site are shown as points in figure 2.9. The solid line represents the "best fit" Saxton equation through these points. The sand and clay contents that yielded this best fit line were 77.5% sand and 17.5% clay. A similar procedure was applied for the Young 1 site, yielding "effective" sand and clay contents of 75% and 14%, respectively. However, because the SPA model uses the same sand and clay content for the different soil layers, these estimates were used to make a first parameterization, and provide a reference to perform a sensitivity analysis to assess the "effective" average sand and clay content of the whole soil profile. After the sensitivity analysis, the final values adopted were 80% sand and 12.5% clay for the old-growth site and 75% sand and 16%clay for the young site.

Root biomass distribution

Root biomass data used by the SPA model correspond to fine roots (less than 1mm in diameter). There are two possibilities to parameterize the SPA model for root biomass distribution. One is entering the values for surface root biomass density (e.g., top 20cm), an estimate of rooting depth and the total root biomass. The root biomass density for the deeper layers is estimated by an

exponential decay function, optimized to fit the parameters entered. The second option is to enter explicitly the root biomass density for all the soil layers.

In this study, I used a mixed approach, because we had data for the root distribution of the upper layers, but not for the whole rooting depth. When digging the soil pits we could observe roots up to 200cm deep. Then, I used the upper 60cm measured data and estimated root biomass for the deeper layers with an exponential decay function, assuming that the total root biomass of the calculated layers was 5% of the biomass up to 60cm. As the root measurements did not discriminate between live and dead roots, I assumed that live roots represented 56% of the total root biomass, in accordance to Jackson (1997).

Soil water content at field capacity

The soil water content at field capacity (draincheck variable within the model) represents the proportion of the total porosity that can be filled by water after gravitational drainage. This value was calculated, in order to fit the maximum stable soil water content measured in the sites (33 % volumetric m^3 m^{-3}). The total porosity was calculated using the respective sand and clay content of the sites in the Saxton equations for porosity. The final draincheck value used was 75% of total porosity.

Capacitance, above ground leaf specific conductivity, and Root resistivity iteration method

To estimate these parameters, several nested sensitivity analysis were performed and compared the goodness of fit against the sapflow measurements with 30 minutes timestep and in a daily basis. Two phases can be differentiated in this fitting process. The first step of this analysis was done visually making big changes in the variables in order to get an idea of a range where the correct values should be. Thereafter, a more rigorous criterion was applied to select the correct values or ranges of the variables. In this second phase, the intervals of variation were narrowed. The goodness of fit indicators were RMSE against the 30 minutes timestep, RMSE against daily values, and an integrated indicator of the regression parameters (I_Index) as described in Mackay et al. 2003. The weights used for the I_Index parameter were 0.5 for the r^2, 0.495 for the slope, and 0.005 for the intercept. The criterion used was a consecutive selection of ranges of parameters following these steps:

- Lowest 15% of RMSE against the 30 minutes measurements.
- Lowest 15% of RMSE against the daily values
- Highest 15% of I_Index against the 30 minutes data.

Results

Sensitivity analysis of SPA

The purpose of this analysis was to determine the relative influence of many of the input variables for SPA on some critical output variables of the model. This information was valuable in the parameterization of the model. More accuracy was required to assign values to variables that had the most influence on model results.

The output variables explored in this analysis were GPP, transpiration, discharge of water from the rooted zone of the soil, evaporation from the soil, run off, and evaporation from wet surfaces. For each input variable, an initial reference value was assigned based on the best information available for the old-growth stand. The reference values were then altered individually by 50% greater and 50% less than the initial value. An exception was height, where a value of 45m (intermediate between the young and old stands) was used as the reference value. The influence of each parameter on a response variable was measured as a percentage of change of the response variable. Values of response variables were calculated as the cumulative value for the period from the end of May (day 82) until the end of October (day 305) of the year 2002.

The ten most influential parameters on GPP are shown in figure 3.1; the influence of these variables on transpiration is also shown. The most influential parameters on GPP were Leaf Area Index (LAI) and minimum leaf water potential (min LWP). Increasing the value of LAI from the reference value minus 50% to the reference value plus 50% caused an increase in GPP of 44%; increasing min LWP over the same range caused GPP to decrease by 28%. The most influential variable on transpiration was above-ground leaf specific conductivity (Gplant), which caused an increase of 84%. LAI caused an increase of 64% in transpiration, and Min LWP caused a decrease of 61%.

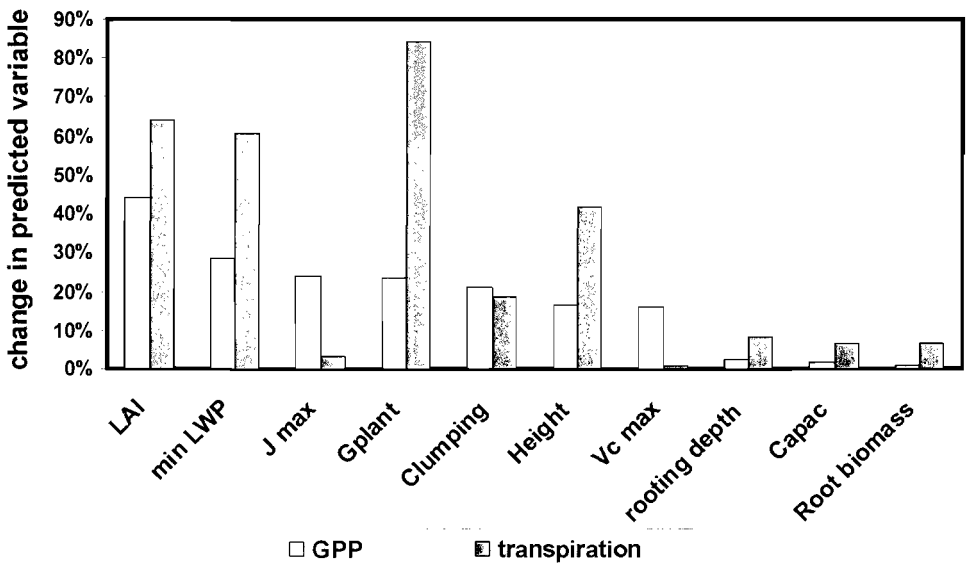

Figure 3.1 – Sensitivity analysis on the scalar input variables of the SPA model (x axis) on the output variables GPP (light blue bars) and transpiration (dark red bars) as absolute percent of change when the analyzed parameter was varied by a total of 200% (50% more and a 50% less of the value used for each parameter on the parameterization for the old-growth stand, except for height where an intermediate value of 45m was used as the reference value).

Variations in the input values for height affected transpiration 3.5 times more than GPP. Of all of the variables examined, the clumping coefficient (which describes the distribution of foliage within canopy layers) had the most similar impact on GPP and transpiration (19% and 21% respectively). The value used for canopy water storage had a large effect on the evaporation from wet surfaces (increase of 77%). The percentage of clay in the soil had a large effect on runoff and discharge of water from the soil. Not surprisingly, the photosynthetic capacity parameters Vcmax and Jmax had a higher impact on GPP (16% and 24% respectively) than on transpiration (1% and 3% respectively). Variations in the input values for rooting depth, capacitance (water storage in plant biomass available for transpiration), root biomass, root resistivity, proportion of rain retained per soil layer (macro porous indicator), leaf dimension, clay percentage, canopy water storage, and throughfall, had an impact of less than 2% on GPP.

Field measurements of sapflow and relationships with environmental drivers

Field measurements of sapflow density were used to parameterize and calibrate the model for a young and an old stand. To understand more about the expected responses from the model, an analysis was conducted of the time series of transpiration, differences in stand-level transpiration in the two stands,

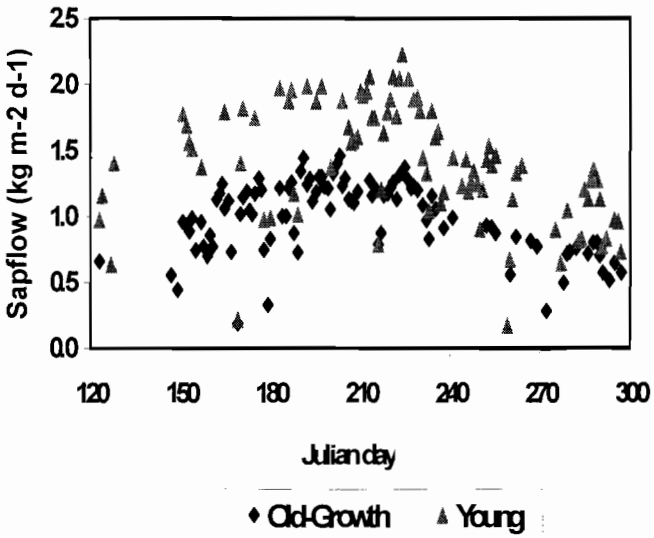

Figure 3.2 – Daily sapflow (transpiration), computed from field measurements of, sapflow density on a daily basis (kg m^{-2} d^{-1}), for the year 2002 (from early May until late October), on an old-growth (blue rhombus) and a young stand (fuchsia triangles).

and relationships between transpiration and environmental drivers (radiation, precipitation, soil moisture).

Over the study period, similar trends were observed in sapflow per unit ground area (i.e., transpiration) for both young and old-growth stands (fig. 3.2). During the spring, (day 120 until 170) sapflow per ground area increased; through the early part of the summer (day 171-230) sapflow "plateaued"; in the last third of the summer (starting around day 230) sapflow steadily decreased until the end of our measurements. Not surprisingly, photosynthetically active radiation (PAR), and vapor pressure deficit (VPD) (fig. 3.3) follow a similar trend as the sapflow measurements.

Over the entire measurement period, the young stand averaged 1.49 times greater daily sapflow density than the old-growth stand (fig.3.4), on a daily basis from the beginning of May to the end of October (days 123 to 297, SE = 0.15 kg m^{-2} d^{-1}).

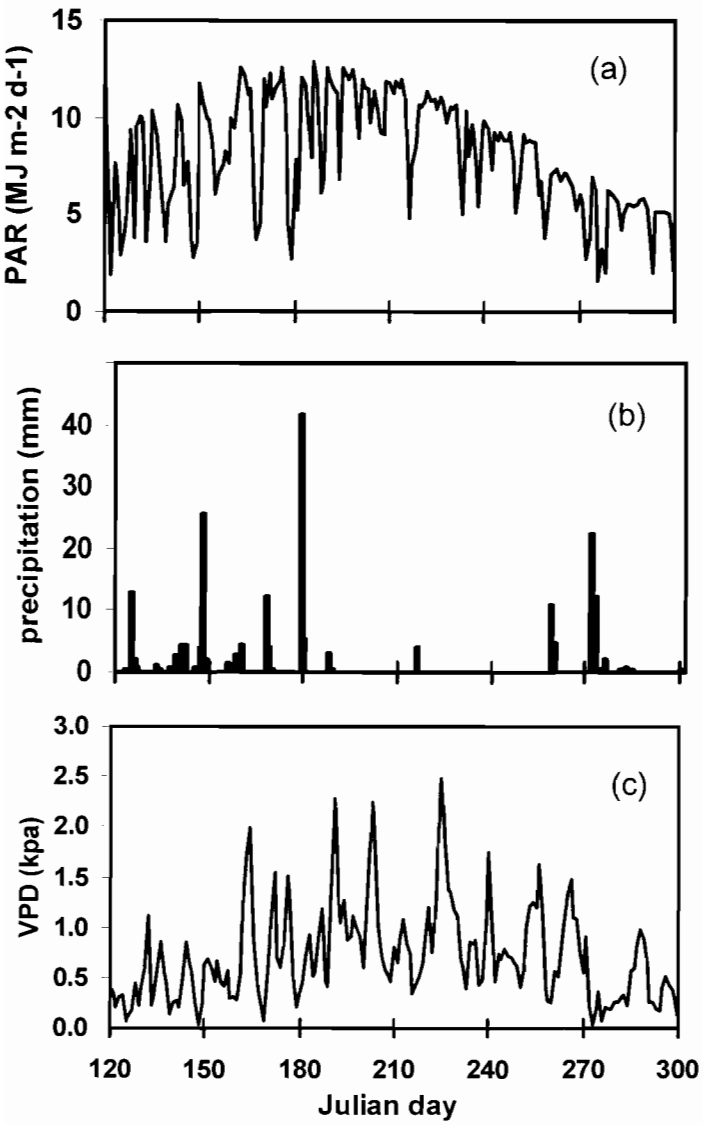

Figure 3.3 - Meteorological drivers (a) Daily total photosynthetically active radiation (PAR, in MJ m $^{-2}$ d^{-1}),(b) daily average vapor pressure deficit (kPa), and (c) daily total precipitation (mm), for the year 2002, from early May until end of October.

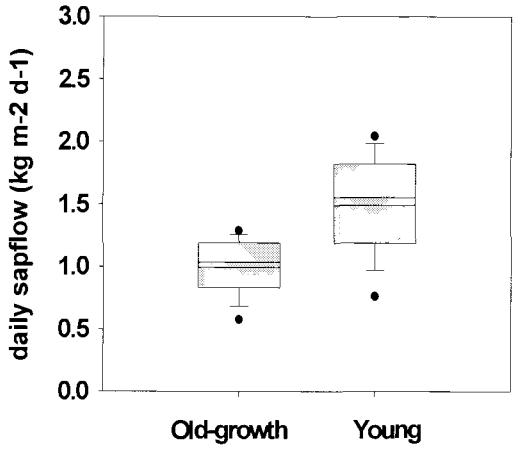

Figure 3.4 - Mean stand daily sapflow (kg m^{-2} d^{-1}) from days 120-300 by site.

The relative change in total sapflow per day per unit ground area over the study period was similar between the young and old-growth stands (fig 3.5).The relative contribution of the different species at each site to the stand-level sapflow per unit ground area was different between sites, mainly due to differences in species composition. In the young site Douglas-fir contributed 91% of the total daily sapflow of the stand; in the old-growth stand the same species contributed only 53% of the total daily sapflow. The percentage of sapflow contributed

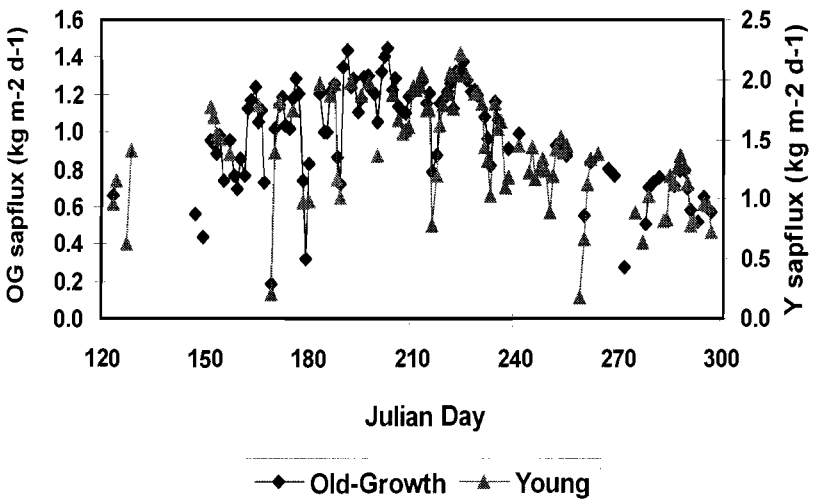

Figure 3.5 - Stand age effect on sapflow density in a daily basis (kg m^{-2} d^{-1}), for the year 2002 (from early May until late October), on an old-growth (blue rhombus) and a young stand (fuchsia triangles). This figure is similar to Fig. 2.4, except that here sapflow for each stand is plotted in a different scale to better visualize the temporal change in sapflow through the measurement period.

by Douglas-fir in the young site equals the percent of leaf area of Douglas-fir on the stand, while in the old-growth stand the relative contribution to total sapflow is almost twice as much as the percent of Douglas-fir leaf area to total leaf area of the stand. In addition, more species contributed to the total sapflow in the old-growth than in the young stand (fig.3.6).

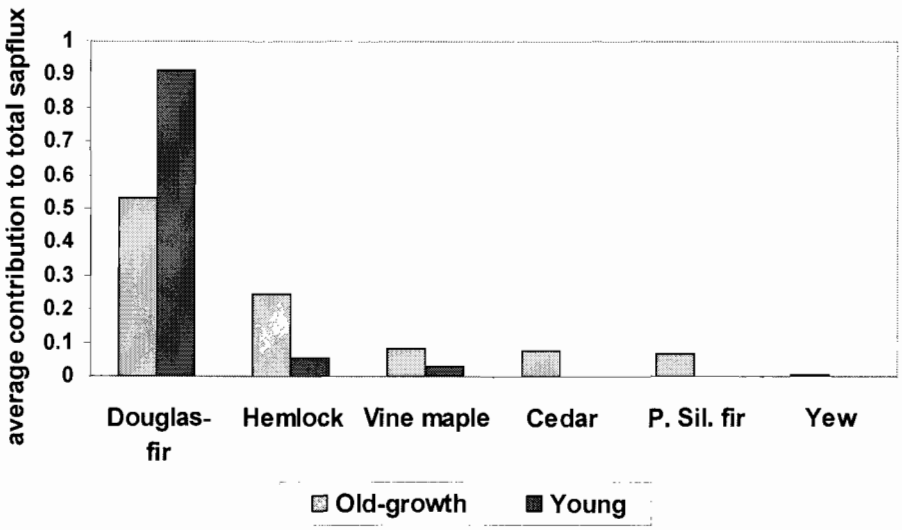

Figure 3.6 - Average contribution per species to the total daily sapflow density per unit ground area of each stand (proportion of the total sapflow density of the stand).

The proportional contribution of the various species on the total daily sapflow per unit ground area differed over time, and describes a different pattern over the study period (fig.3.7). The proportional contribution of Douglas-fir was nearly constant over the season in the young stand (91%, SE = 0.1%). In the old-growth stand Douglas-fir was also the main contributor to the total sapflow of the stand, but the proportion of its contribution changed through the season. From the beginning of March (day 58) until the beginning of May (day 120) the

average contribution of Douglas-fir to stand-level sapflow was 62% (SE = 1.2%). In the middle of the season, the proportional contribution of other species increased; thus, the average proportional contribution of Douglas-fir at this time decreased to 48% (SE = 0.5%, days 120 until 240). After the end of August (day 240) the relative contribution of Douglas-fir to total sapflow increased again to average 56% (SE=1.1%) of the total sapflow of the stand between days 240 and 301. In the old stand but not the young, there was considerable day-to-day variation in the proportional contribution of Douglas-fir to stand-level sapflow (note the blue points that fall above the overall trend in Fig. 3.7a). These apparent "outliers" occurred on cloudy or rainy days, suggesting that transpiration of Douglas-fir is comparatively greater than the other species in humid, light-limiting conditions.

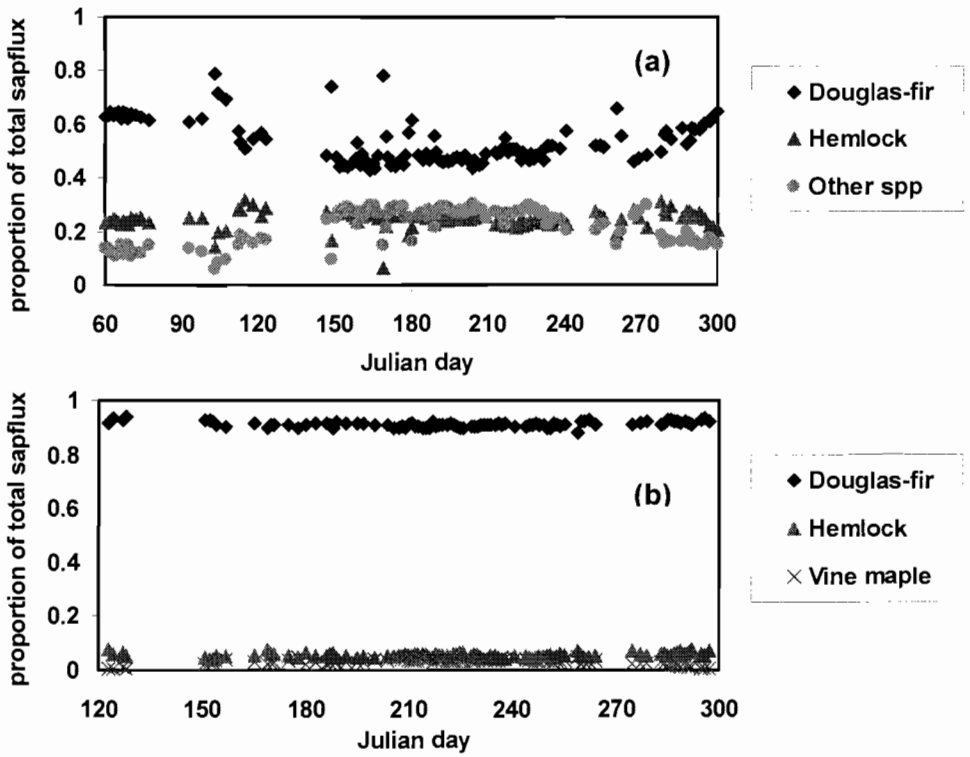

Figure 3.7 - Relative contribution of the different species present in each stand to the daily total sapflow density per unit ground area of the stand. (a) Old-growth stand, other spp. corresponds to cedar, pacific silver fir, yew, and vine maple. (b) Young stand, all the species measured are represented in the plot. Note the different time scale, due to the lack of measurements in the young site before the day 120.

Fit of the SPA model against sapflow density

The model was tested against both half-hourly and daily estimates of sapflow per unit ground area. These estimates were derived from measurements of sap velocity and scaled from individual sensors to the stand level of both young and old-growth stands of Douglas-fir/western hemlock forest as described in the

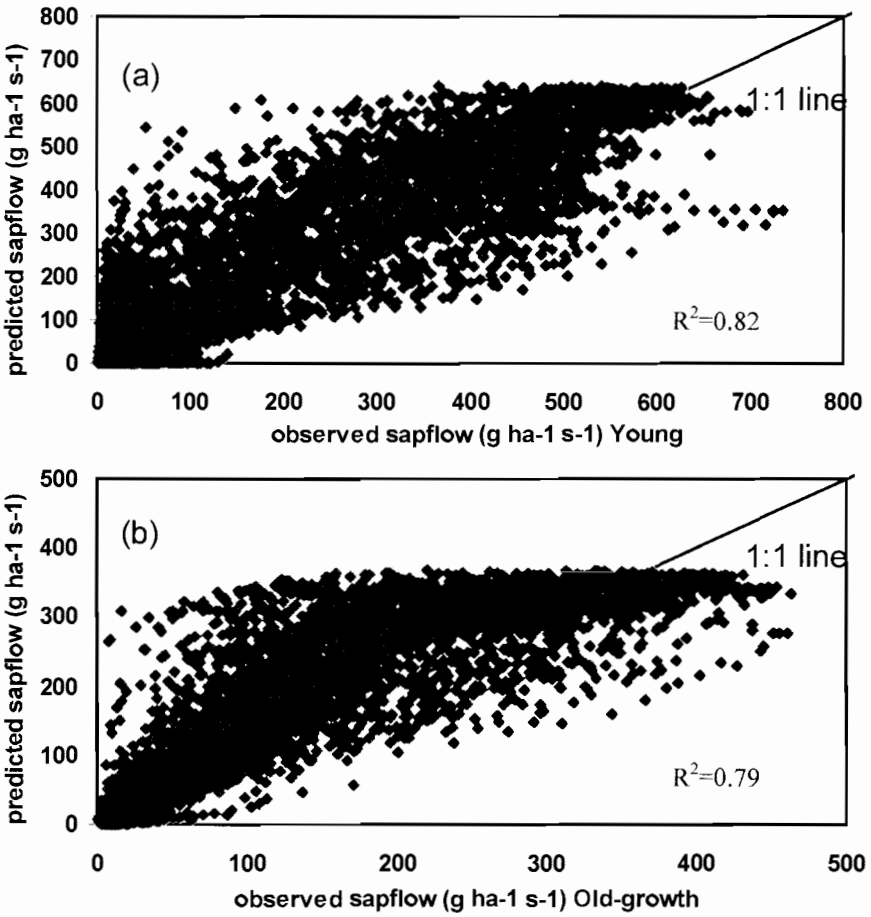

Figure 3.8 - Observed vs. predicted by the SPA model stand total sapflow density (g ha-1 s-1), in 30 minutes timestep, for the year 2002. (a) Young stand. (b) Old-growth stand

Methods section. The parameters for the SPA model were derived from field measurements when they were available, or calculated through an iterative process in order to get the best fit against sapflow measurements.

From a regression analysis of predicted against observed half hourly measurements of sapflow density (fig. 3.8), the r^2 values were 0.82 (slope 1.004) for the young site, and 0.79 (slope 0.973) for the old-growth site. It can be seen in the plot of observed vs. predicted sapflow data on a half hourly basis of the old-growth stand (fig.3.8.b) that predicted values reached a plateau while the observed values continued to increase. A possible explanation for this pattern is that the model misrepresents the stomatal control on transpiration of species other than Douglas-fir. It has been shown previously that western hemlock, which is a shade tolerant species that contributes 40% of the total leaf area, has higher stomatal conductance than Douglas-fir under high levels of vapor pressure deficit (Waring and Franklin 1979).

In addition, the model does not account for the effects of gaps in the forest stand. Gaps are an important trait of mature stands and play an important role in the light regime of understory species. Therefore, during midday the difference between predictions and measurements should be greater because the understory species are receiving direct sunlight.

When comparing the model results against the daily sapflow density values, the r^2 values were 0.79 for the young site, and 0.755 for the old growth site. Over the study period the model tended to overestimate observed sapflow measurements at the beginning and at the end of the season in the old-growth stand, while in the young stand there was only a short period in the beginning of the summer where the model overestimated total daily sapflow density per unit ground area (fig. 3.9). This same effect can be seen when the model predictions are plotted against half hourly measurements in a time series (fig.3.10), where it can be observed that the misrepresentation of the model occurs at the middle of the day. The measured and modeled sapflow in the "tails" of half-hourly data (i.e., the curves at the beginning and end of each day) are well matched, indicating that the model simulated quite well short-term water dynamics dependent on

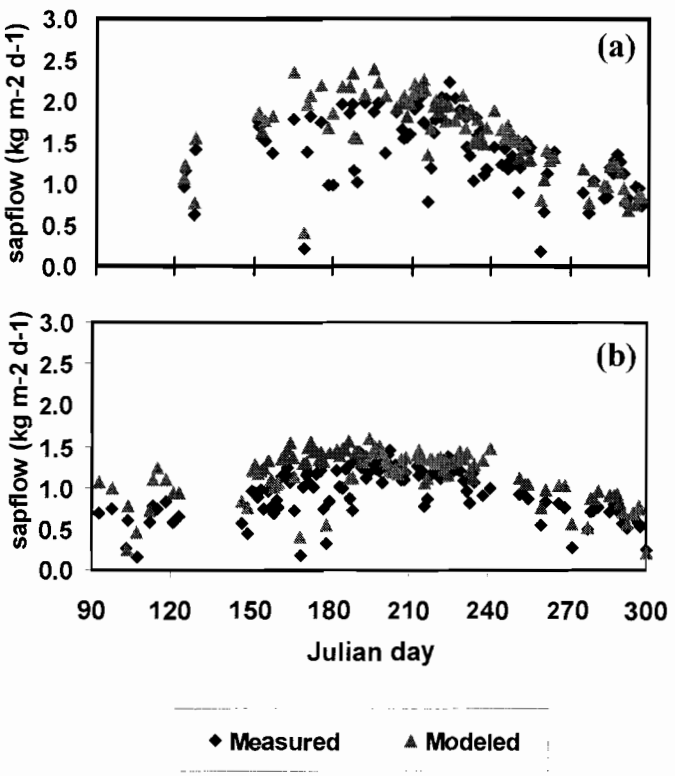

Figure 3.9 – Modeled and measured sapflow density (kg m-2 d-1) on a daily basis, for the study period of 2002 (a) young Douglas-fir stand, (b) old-growth Douglas-fir/western hemlock stand. Blue rhombus represents the measured data, and fuchsia triangles the model prediction.

plant conductivity and capacitance, which were the variables fitted through an iterative process.

Not surprisingly, the variance of the sapflow measurements and predictions are twice as much for the young site than for the old-growth site. As the hydrological restrictions are smaller in the smaller trees, the potential for transpiration is higher. Then, when there are limiting meteorological conditions they will decrease transpiration of both stands in a similar rate, but the young stand would decline from a higher maximum. However, the differences between variances are higher than the differences between means, suggesting a resiliency increase in the old-growth stand due to the structural and physiological changes.

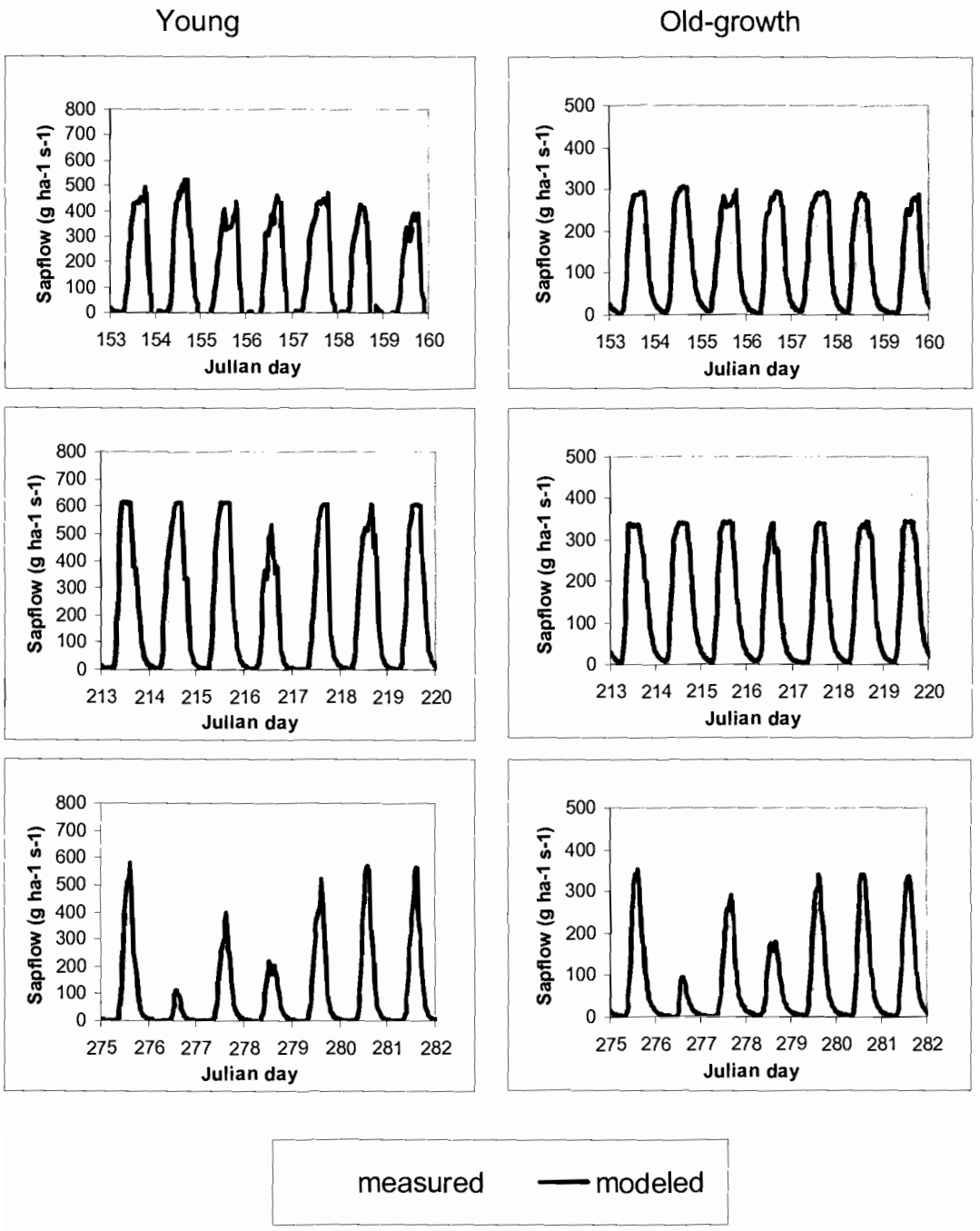

Figure 3.10 - Detailed sapflow density (g ha^{-1} s^{-1}) and model predictions, in 30 minutes timestep, for three different weeks on the growing season (early June, end of July – beginning of August, and beginning of October). The fuchsia line represents the measured data, and the blue line the prediction of the model. Note the different scale between the two sites.

Using the fitted model to test hypotheses and make predictions

Over the entire study period (from late March, until the end of October, Julian days 82 until 305) the model predicted the following cumulative differences in processes between the young and old stand: The young site had 1.3 times greater transpiration than the old growth site, 1.37 times greater soil water depletion, 2.9 times greater runoff, and 1.14 times higher latent energy flux (fig. 3.11). Unexpectedly, GPP and discharge of water from the rooted zone (leaching) of the soil were predicted to be similar over the whole period (1% and 7% lower in the young site respectively). Soil evaporation, and evaporation from wet surfaces were predicted to be higher in the old-growth stand than in the young stand, 1.17 and 1.67 times respectively

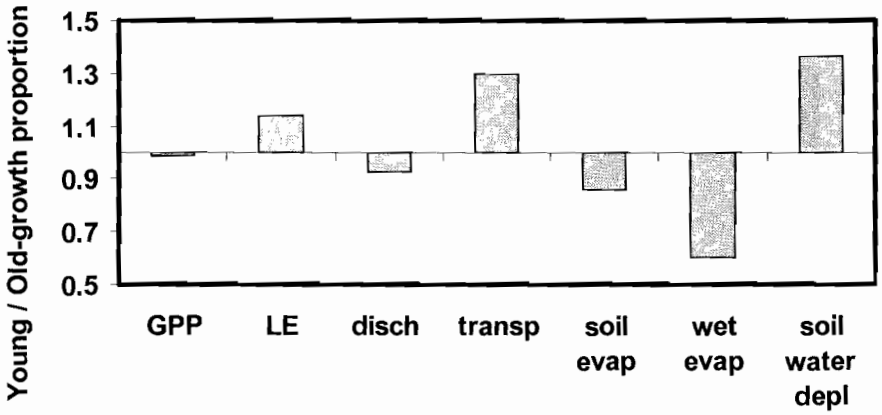

Figure 3.11 – Ratio between predictions of the model for the young and the old-growth stands for cumulative output variables from late March until the end of October (days 82 to305), for the year 2002.

Structural and physiological differences between young and old-growth Douglas-fir / western hemlock stands: sensitivity analysis to assess functional implications.

There were many structural and physiological differences between the young and old stands. Also, as noted previously, minimum leaf water potential is lower in the old growth stand (McDowell et al. 2002b) and capacitance is greater in large trees (Phillips et al. 2002). It has been suggested that the lower minimum water potential and higher capacitance may partially "compensate" for the potential limitations of large size to transpiration (McDowell et al. 2002b). A benefit of a detailed physiological model such as SPA is that it allows researchers to investigate the individual impacts of these variables on overall stand function, although one must be cautious about these interpretations.

SPA was used to examine several of the structural and physiological variables that were found to be different between the old-growth and the young site. Some of these variables were measured directly; others were derived through the optimization process of model fitting discussed in the Methods section. Tables 3.1 and 3.2 identify these variables and the values used in this thesis for the model runs of young and old stands.

	OG	Y1	Units
Height	61.3	17.5	m
min LWP	-2.6	-2.1	Mpa
Vcmax	32.53	26.3	μmol m-2 s-1
Jmax	98.04	74.73	μmol m-2 s-1
Canopy water storage	3.32	1.11	Mm
Throughfall	0.36	0.12	Ratio (mm/mm)

Table 3 - Scalar Variables measured different in between sites

	OG	Y1	Units
Above ground LSC	1.75	0.9	mmol m-1 s-1 MPa-1
Capacitance	650	625	mmol m-2 LA MPa-1
Root Resistivity	10	25	MPa s g mmol-1

Table 4 - Variables fitted through optimization process

Height

In these analyses the model was run multiple times with all parameters except for height maintained constant and set to the values used for the old-growth stand. Height was varied incrementally from the young site value (17.5m) to the old-growth value (62.5m). This change in height caused reductions of 43% and 17%, respectively, in total transpiration and GPP summed over the study period (fig.3.12 (a)). In a parallel set of model runs, all of the parameters other than height were set to the valued used for the young stand, and again height was increased incrementally. In this case the increase in height caused a reduction of 49% and 25% in the total transpiration and in GPP respectively over the study period (fig.3.12 (b)).

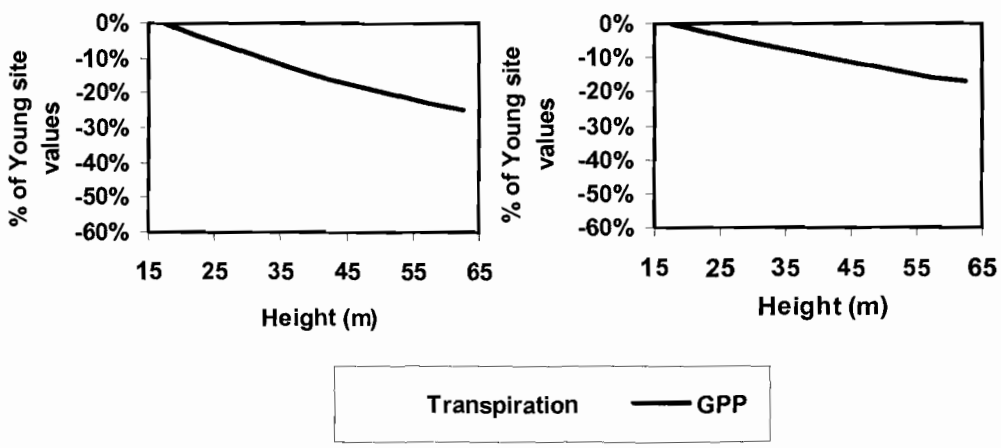

Figure 3.12 – Sensitivity analysis for height – Change in transpiration (fuchsia line) and GPP (blue line) as a percentage of the value predicted when height had the young site value (17.5m) for the year 2002, from late March until the end of October (days 82 until 305). In (a) all the parameters except for height are kept constant with the parameterization values for the old-growth stand, while in (b) the values used correspond to the parameterization values for the young stand.

Above ground leaf specific conductivity

Above ground leaf specific conductivity can be a difficult concept to grasp for those unaccustomed to hydraulic properties of trees. The "specific conductivity" of a piece of tissue is more or less analagous to its permeability, and is mostly a function of anatomical properties of the xylem (larger cells result in higher conductivity). At any point along the hydraulic path, the "conductivity" at that point is equal to the specific conductivity multiplied by the cross sectional area. The average conductivity of the whole tree is the mean value of conductivity at all points along the path. Finally, above-ground leaf specific conductivity (at least as used in SPA) is the average conductivity of all above-ground tissues divided by the total leaf area.

The impacts of varying leaf specific conductivity on seasonal transpiration and

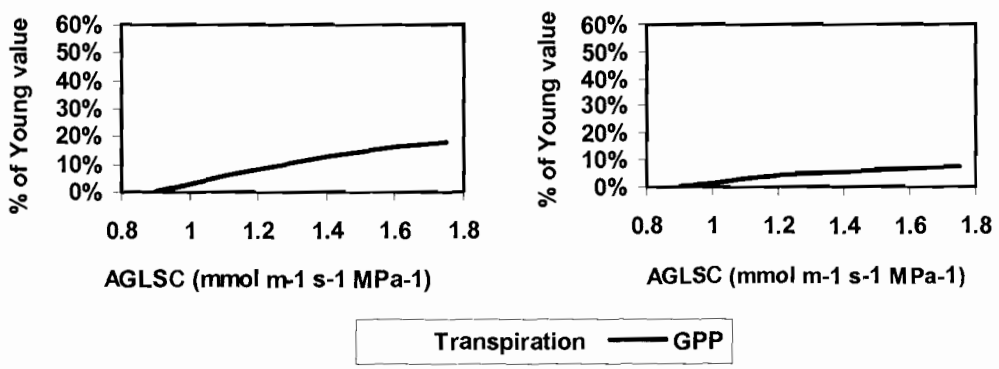

Figure 3.13 – Sensitivity analysis for AGLSC – Change in transpiration (fuchsia line) and GPP (blue line) as a percentage of the value predicted when above ground leaf specific conductivity (AGLSC) had the young site value for the year 2002, from late March until the end of October (days 82 until 305). In (a) all the parameters except for AGLSC are kept constant with the parameterization values for the old-growth stand, while in (b) the values used correspond to the parameterization values for the young stand.

GPP (fig. 3.13) was evaluated using an approach similar to the evaluation of height above. First, all paramenters were set to the values of the old growth site, and above-ground leaf specific conductivity was varied incrementally from the value determined by the optimization process for the young site (0.9 mmol m-1 s-1 MPa^{-1}) to the value determined for the old site (1.75 mmol m^{-1} s^{-1} MPa^{-1}). Then the process was repeated using the parameter set for the young site.

Minimum leaf water potential

The change in minimum leaf water potential (Ψ_L min) showed a similar trend as the change in AGLSC. The modification in Ψ_L min from the young site value (-2.1 MPa) to the old-growth value (-2.6 MPa) caused an increase of 12% and

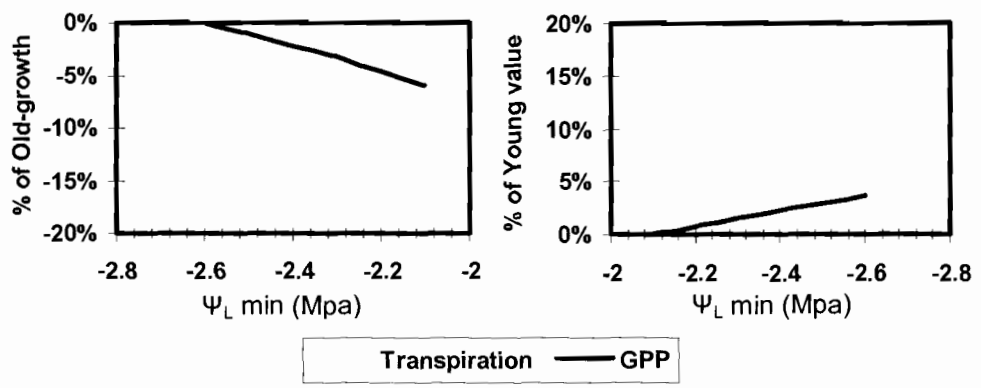

Figure 3.14 – Sensitivity analysis for Ψ_L min – Change in transpiration (fuchsia line) and GPP (blue line) as a percentage of the value predicted with the original parameterization for each site for the year 2002, from late March until the end of October (days 82 until 305). Ψ_L min was changed from the young value (-2.1 MPa) to the old-growth value (-2.6 MPa). In (a) all the parameters except for Ψ_L min are kept constant with the parameterization values for the old-growth stand, while in (b) the values used correspond to the parameterization values for the young stand.

4% in the predictions of total transpiration and GPP, respectively, for the young site set of parameters (fig.3.14 (b)), and a decrease of 16% and 6% in the total transpiration and GPP respectively, in the old-growth stand (fig.3.14 (a)).

On absolute values, the modification in Ψ_L min from the young site value to the old-growth caused a compensational increase of 84 gC m-2 in GPP, and 39mm in transpiration (cumulative for days 82 until 305, year 2002).

Root resistivity

The impact on GPP and transpiration due to a change in root conductivity on a biomass basis was minor compared to the effect of height, AGLSC, and Ψ_L min. The increase in root resistivity from the young site (5MPa s g mmol^{-1}), to the old-growth site value, caused a decrease of 2.2 % in transpiration and 0.4% in GPP (fig.3.15).

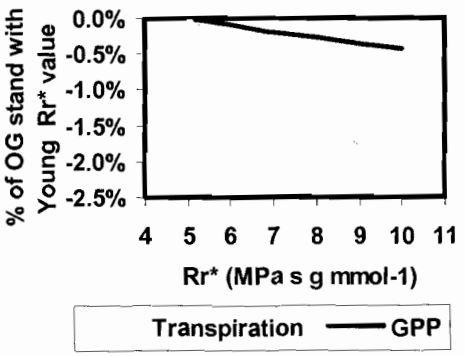

Figure 3.15 – Sensitivity analysis for Root resistivity Rr* – Change in transpiration (fuchsia line) and GPP (blue line) as a percentage of the value predicted for the old-growth site, when root resistivity had the young site value (5 MPa s g mmol^{-1}).

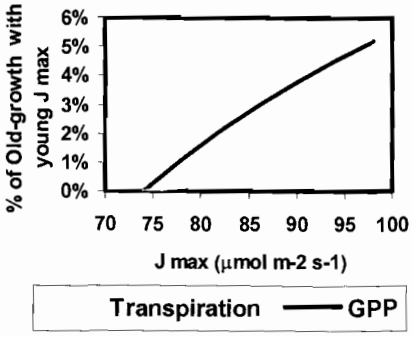

Figure 3.16 – Sensitivity analysis for Jmax - Change in transpiration (fuchsia line) and GPP (blue line) as a percentage of the value predicted for the old-growth site, when Jmax had the young site value (74 μmol m^{-2} s^{-1}).

Photosynthetic capacity

Not surprisingly, the change in photosynthetic parameters had a greater impact on GPP than on transpiration. However, the effect was secondary compared to other variables like height, AGLSC or Ψ_L min.

The individual analysis on Rubisco maximum carboxylation capacity (Vcmax) yielded an increase of 2.3 % of GPP for the old-growth site (31gC m^{-2}),while the change in maximum rate of electron transport (Jmax) from the young to the old-growth stand caused an increase of 5.2% on GPP (69.2 gC m^{-2}; fig.3.16).

Throughfall and Canopy Storage of Rainfall

The effect of maximum canopy water storage (CWS) and throughfall on GPP was negligible. The effect of CWS on transpiration was less than 1% in the old-growth stand, and 2% in the young. Throughfall effect on GPP and transpiration was lower than 0.1%

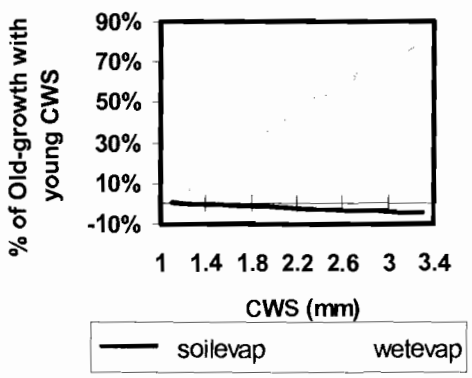

Figure 3.17 – Sensitivity analysis for canopy water storage - Change in evaporation from wet surfaces (wetevap, light blue line) and soil evaporation (soilevap, dark blue line) as a percentage of the value predicted for the old-growth site, when CWS had the young site value (1.1 mm).

in all the cases. However, the modification of CWS and direct throughfall from the young site to the old-growth stand caused a shift in the partition of water among different components of the water budget. The most important change was observed on the evaporation from wet surfaces on the canopy (wetevap). When CWS was changed from young site (1.14mm) to the old-growth site value (3.32mm) evaporation from wet surfaces (wetevap) increased by 80% (fig. 3.17), or 22mm in absolute values.

Leaf area distribution

Model predictions for the structural change in vertical distribution of the leaf area (LAVD) suggested that the shift towards old-growth stand LAVD produced an increase in water use efficiency. Running the model with the parameterization for the old-growth site but the LAVD of the young stand, predicted an increase of 13% in transpiration, and a decrease of 2.5% in GPP, compared with the predictions for the same site with the old-growth LAVD. On the other hand, replacing the LAVD on the young stand with the old-growth site LAVD caused a decrease of 6.2% in transpiration, and an increase of 2.4% in GPP (fig.3.18).

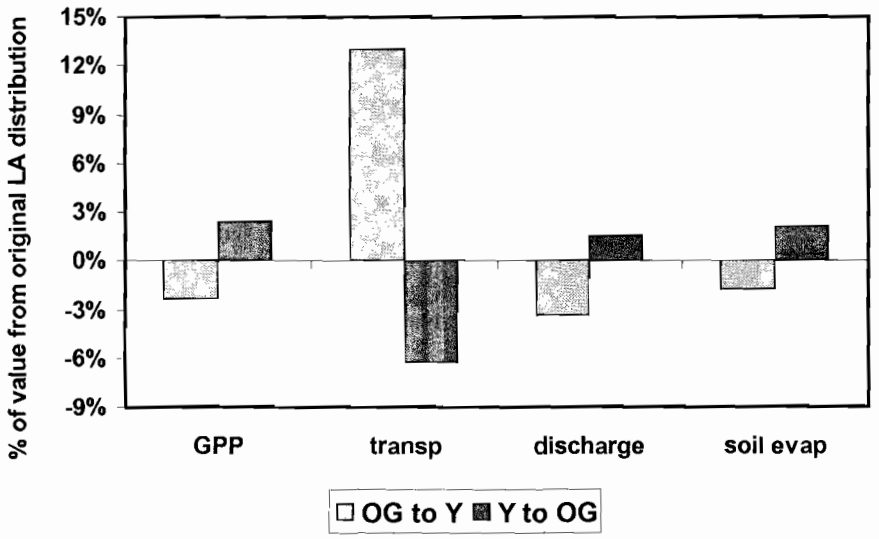

Figure 3.18 – Effect of leaf area vertical distribution (LAVD) on different response output variables of the SPA model. "OG to Y" is plotted as the proportional difference between the old-growth site with the young stand LAVD, and the original parameterization for the old-growth stand. "Y to OG" is the difference for the young stand, when the LAVD was changed with the old-growth values.

Root distribution

The modifications of root distribution on a biomass basis between the young and the old-growth sites had a minor impact on GPP and transpiration. The main impact on a percentage change basis was observed on soil evaporation and discharge of water from the rooted zone of the soil (fig.3.19). However, the root vertical distribution of both sites was very similar.

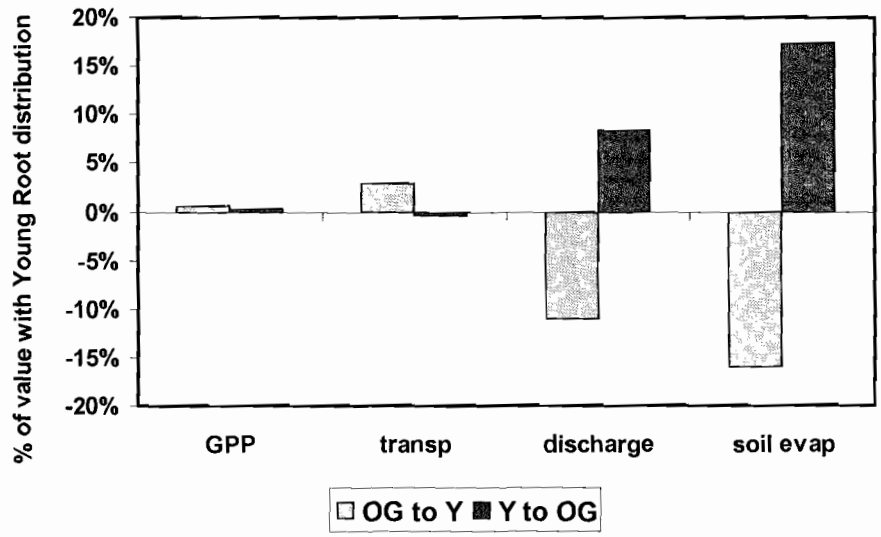

Figure 3.19 – Effect of root biomass distribution on different response output variables of the SPA model. "OG to Y" is plotted as the proportional difference between the old-growth site with the young stand root distribution, and the original parameterization for the old-growth stand. "Y to OG" is the difference for the young stand, when the root distribution was changed with the old-growth stand values.

Discussion

The first objective of this study was to adapt a computer simulation model of forest processes to a young (25year old) and an old-growth (450-500 year old) Douglas-fir/western hemlock forest stand in order to predict fluxes between them and the atmosphere. Measured values of water fluxes were used to calibrate the model. The second objective was to use the calibrated model to estimate carbon fluxes or gross primary productivity. The third objective was to use the model to quantify the effect of the variables found different between stands of different developmental stages on carbon and water fluxes. The fourth and final objective was to improve the versatility of the model software and make it available to other researchers for use in additional types of forests. Modifications of the model interface make it more accessible to other users.

I. Adaptation of the SPA model to young and old Douglas-fir/western hemlock forests

The model predicted transpiration adequately for both young and old-growth stands. Nevertheless, the accuracy of the predictions in the old-growth stand varied throughout the growing season. In the early and late season the model overestimated stand transpiration, while in the middle of the season underestimated the measurements (fig. 3.10.b). This variation in the fit appears to be due to the increased complexity of the old-growth stand, where different

species are contributing more to the total transpiration of the stand than in the young stand.

As SPA is currently configured, there is a single set of physiological parameters for the forest stand. In a multi-species stand, this set of parameters represents the average of all species. As long as the relative contribution of these species does not change through time and space, there is no problem with using the "average conditions" for modeling. However, the relative contribution of various species to transpiration changed through the season in the old-growth stand (fig. 3.8). In addition, it can be seen in the plot of observed vs. predicted sapflow data on a half hourly basis of the old-growth stand (fig.3.9.b) that predicted values reached a plateau while the observed values continued to increase. A possible explanation for this pattern is that the model misrepresents the stomatal control on transpiration of species other than Douglas-fir. It has been shown previously that western hemlock, which is a shade tolerant species that contributes 40% of the total leaf area, has higher stomatal conductance than Douglas-fir under high levels of vapor pressure deficit (Waring and Franklin 1979). All of this suggests that the set of parameters used for the old-growth stand should have varied through the season in order to accurately represent the shift in species contributing to the total transpiration of the stand. This variation was not incorporated into the model for this thesis because there was no unbiased way to change the parameterization, and SPA is not currently set up to easily change the parameter set over time.

II. Using the parameterized model to predict gross primary productivity (GPP) for young and old Douglas-fir/western hemlock forests.

The SPA model was selected for this study because of its unique detailed physiological approach that incorporates hydraulic limitations to transpiration and stomatal conductance and its explicit link between stomatal conductance and photosynthesis. This model was previously applied to a broad variety of ecosystems and it successfully predicted GPP and transpiration as measured by eddy covariance (Williams et al. 1996, Williams et al. 1998, Law et al. 2000, Williams et al. 2001). Therefore, I was expecting to get adequate estimates of GPP after parameterizing the model against sapflow data.

To test the reliability of the GPP estimates for the study sites, I compared them against estimates of stem wood growth efficiency per leaf area calculated for the same sites in earlier studies (McDowell et al. 2002), and against other measurements during to the same period (Ocheltree unpublished data). As the total leaf area of the sites under study was equal, the ratio between the estimates of stem wood production (SWP) for both sites (SWP_{young}/ SWP_{old}) was assumed to be equal to the ratio between above-ground net primary production (AGNPP) at the two sites ($AGNPP_{young}$/ $AGNPP_{old}$). Net primary production (NPP) has been proposed to be a constant fraction of GPP (Waring et al. 1998). Therefore, if the proportion of NPP allocated belowground remains

constant with age, the ratio between $AGNPP_{young}$/ $AGNPP_{old}$ should be equal to the ratio GPP_{young}/GPP_{old}. (Note however that this assumption contradicts the hypothesis of Magnani et al. (2000) that the proportion of photosynthate allocated belowground increases in older forests). In this study, the ratio, $AGNPP_{young}$/ $AGNPP_{old}$ (derived from direct measurements of biomass and annual wood increments) was double the ratio between GPP_{young}/GPP_{old} (predicted from SPA) , suggesting an overestimation of GPP by the model in the old-growth stand. A possible explanation for this overestimation of GPP in the old-growth stand is that the parameterization of the model was done using data available for Douglas-fir, and stand-average estimates of hydrological parameters. This procedure is reasonable for the hydrologic phase of the modeling approach, where Douglas-fir is the major contributor to the total transpiration of the stand, but the same species only contributes 28% of the total leaf area of the stand. The other species present in the stand are shade tolerant and probably have less growth efficiency per leaf area than Douglas fir. It would be reasonable to expect that SPA would predict lower GPP if parameters for photosynthetic capacity (Vcmax, Jmax) were averaged for all species. However, although the optimization procedure used in parameterizing the model automatically fit "stand average" values for some variables directly involved in transpiration (such as leaf-specific conductivity), the values for photosynthetic capacity came from direct measurements of sun foliage in Douglas-fir.

In addition, in the young stand there was an infection of Swiss Needle Cast (SNC) that caused a reduction in stomatal functionality of young Douglas-fir (Dr. Julia Kerrigan, personal communication). This infection could lead to reduced overall stomatal conductance, and thus, carbon assimilation. However, the reduction in carbon assimilation would not be observed completely in the growth efficiency values, because they are averages of the last five years, and the infection appears to be recent. Therefore, parameterizing the model with the current conditions of infection could result in an underestimation of GPP of uninfected Douglas fir stands. I want to point out, that even if the effect of SNC occurs at the vapor phase level, the consequent reduction in transpiration leads to a reduction in the AGLSC parameter of the model. Consequently, the fitted value for AGLSC of the young stand may not represent the potential conductivity lead by the structural characteristics of the young Douglas-fir trees.

Other potential effects on the performance of the model are discussed later under "misrepresentations of the SPA model".

III. Quantification of the effects of the variables found different between stands of different developmental stages on carbon and water fluxes

Recently, there has been much controversy regarding the causes of age-related decline in forest productivity (Ryan and Yoder 1997, Ryan et al. 1997, Magnani et al. 2000, Becker et al. 2000, Battaglia 2001, Binkley et a. 2002, Ryan et al. in press). The classic explanation for this decline is that photosynthesis reaches a plateau as leaf area stops increasing, and subsequent increases in the amount of biomass leads to an increase in respiration. However, there is evidence of net photosynthesis decline as stands age, or individual trees grow taller (Yoder et al. 1994, Hubbard al.1999). Also, there is experimental evidence that does not support the increasing respiration hypothesis as the cause of growth decline (Ryan and Waring 1992). A variety of alternative explanations were stated to explain the age-related decline in productivity:

Hydraulic limitation hypothesis. As height increases, leaf specific hydraulic conductance (k_l) and stomatal conductance (g_s) decline, and thus, carbon assimilation would also decrease (Yoder et al. 1994, Ryan and Yoder 1997).

Nutrient immobilization. The availability of nutrients may decrease as they accumulate in biomass (Binkley et al. 1995).

Allocation changes. Increased belowground allocation to increase the fine roots to foliage ratio (Magnani et al. 2000). Increased allocation to reproductive structures causing a reduction in wood production (Ryan et al. 1997 after Linder and Troeng 1981).

Genetic maturation of meristems. Genetic expression on meristems may change with tissue age and cell divisions (Ryan et al. 1997 after Greenwood and Hutchinson 1993).

The modeling approach of this study allowed me to quantify the individual impact of each variable found to be different between the young and the old-growth stands of Douglas-fir/western hemlock forest. By identifying the sensitivity of water and carbon fluxes to the range of natural variation found in these variables, it is possible to examine the likelihood of the various hypotheses presented above. However, the conclusions that can be drawn from the model runs are constrained by the assumptions built into the model's algorithms, discussed later, and the scale at what it was designed to work. SPA is a stand-level model, and it is not a model of a sum of individual trees. The variables described below correspond to averages of each stand as they are used in SPA.

Maximum height. Among all the variables analyzed, maximum height was the most important variable affecting both transpiration and gross primary production (GPP). Moreover, maximum height increase was the only change

from the young to the old-growth stand that had a considerable *negative* impact on transpiration and GPP. Root resistivity had also a negative impact, but the consequent decrease in transpiration was less than 2.5% and the effect on GPP was negligible. The change of the other variables from the young to the old-growth stand appears to be compensating for the potential negative impact of the increase in height. Under the assumptions made by this modeling approach, the structural and physiological changes as the stand ages achieved a total compensation on GPP and a partial compensation on transpiration (old-growth had 23% less transpiration than the young stand). These results partially agree with the hydraulic limitation hypothesis in the sense that height was the most important factor limiting photosynthesis and transpiration. As there was compensation for the hydraulic constraints imposed by the growth in height, the expected decline in productivity of the old-growth stand (as determined from ground-based measurements of biomass and biomass increments) could not be accounted for by the increase in height.

Above-ground leaf specific conductivity (AGLSC). The modification of this parameter from the young to the old-growth stand had the largest compensatory effect on the potential hydraulic limitation imposed by the growth in height (62% of the decrease in GPP was compensated by changes in AGLSC from the young to the old-growth stand). AGLSC represents the average hydraulic conductivity of all above-ground tissues divided by the total leaf area. Changes in this variable may be due to changes in the leaf area to

sapwood area ratio or sapwood permeability, and both of these parameters can be affected by changes in species composition. AGLSC of the old-growth stand was almost double (1.95 times greater) the value for the young stand. (It is important to note that these values were not measured directly; instead, they resulted from the optimization procedure used to select the best set of variables that could not be measured directly). Mencuccini and Magnani (2000) have proposed changes in sapwood permeability to compensate for the hydraulic limitation imposed by height, and others (Domec and Gartner 2002, Reid et al. 2003) have reported increased sapwood permeability in basal xylem of old vs. young trees). Mencuccini and Magnani (2000) pointed out that this change in permeability represents a cost for the plant by increasing vulnerability to cavitation. However, there is some uncertainty about this prediction. Measured vulnerability curves for branch wood of Douglas-fir indicates that there is very little potential for cavitation near the normal water potentials experienced by this species (e.g., Kavanagh et al. 1999). However, Domec and Gartner (2001; 2002) found that bole-wood was much more vulnerable to cavitation. The shade tolerant species that replace Douglas-fir in the old-growth stand are not likely to have a greater sapwood permeability than Douglas-fir, although these values have not yet been measured. A decrease in the leaf area to sapwood area ratio has been documented as trees grow taller/older (Mc Dowell 2002a). However, the shade tolerant species, which contribute most of the leaf area in the old growth stand, have a higher leaf to sapwood area than Douglas-fir.

Then, the change in species composition would compensate at the stand level for the change in the L_A/S_A ratio of Douglas-fir tall trees. Therefore, I expect that the change in AGLSC of the stand is a consequence of a combined effect of the L_A/S_A ratio, species composition and sapwood permeability changes. Moreover, an indirect effect of the SNC infection could be expected.

Minimum leaf water potential ($\psi_{l\ min}$). It has been shown that many tree species have a midday ψ_{lmin} threshold in order to prevent xylem embolism (Jones and Sutherland 1991). Lower ψ_{lmin} values were measured in taller/older Douglas-fir trees than in shorter/younger trees. This has been proposed as a mechanism to compensate for increased hydraulic resistance caused by increased height (McDowell 2002b, Barnard and Ryan 2003). Having a lower ψ_{lmin} would allow the plant to have stomata open for longer periods of time. Varying this parameter in the model from the young to the old-growth stand values, supported the idea of ψ_{lmin} as a compensatory mechanism for taller trees, and predicted a 24% compensation of the decrease in GPP caused by the increase in height. It is possible that the decreased ψ_{lmin} incurs a "cost" of increased xylem cavitation and reduces conductivity. As SPA is currently configured, leaf-specific conductivity does not vary, and there is no capacity for xylem cavitation. Indeed, little information is currently available to indicate

whether cavitation occurs regularly in Douglas-fir and whether it is more common in large, old trees than in small, young trees.

Roots. Magnani et al. (2000) proposed an alternative hypothesis to explain age-related decline in forest stands. They suggested that as trees grow taller and hydraulic resistance increases, a mechanism to counterbalance this could be an increase in the ratio of fine roots to foliage. This would also lead to an increase in root respiration and root turnover that could explain in part the decline in above-ground growth rate. The results of this study do not support the hypothesis proposed by Magnani et al. (2000). Measurements showed that fine root biomass density up to a depth of 1.2m on these two sites was slightly greater in the young than in the old-growth stand (799.2 g m^{-2} and 693.6g m^{-2} respectively; Kate George unpublished data). The modeling analysis also suggested that the effect of root resistivity and fine root biomass distribution was minor compared to the effect of height, AGLSC, and ψ_{lmin} on both GPP and transpiration. These suggest that an age-related decline in productivity is not likely to be caused by a shift in the above to below-ground carbon allocation.

Photosynthetic capacity. Leaf photosynthetic capacity is strongly related to nitrogen nutrition. Therefore, if nitrogen immobilization occurred this would lead to a decrease in photosynthetic capacity of old trees. This mechanism has been proposed as one of the factors limiting productivity of forest stands (Binkley et al. 1995). The differences found in this study between leaves of old-growth and

young trees indicate an opposite effect. Although nitrogen concentration measurements were not used for the parameterization, both Rubisco maximum carboxylation capacity (Vc_{max}) and maximum rate on electron transport (J_{max}) from full sunlit leaves of dominant trees were higher in the old-growth than young stand. In other studies it has also been shown that the decrease in productivity was not related to a change in photosynthetic capacity of larger trees (Hubbard et al. 1999, McDowell et al. 2002b). The nutrient immobilization hypothesis is not supported by the results of this study. However, the photosynthetic capacity measurements were done on Douglas-fir trees and the stand level effect may be different after accounting for the change in species composition between stands. So although the nutrient limitation hypothesis itself may not account for the age-related decline in productivity, it is possible that lower intrinsic photosynthetic capacity in shade-tolerant species may impact productivity. This potential impact was not included in the modeling exercises in this thesis.

Capacitance. Capacitance, or stored water capacity, is defined as the ratio of change in tissue water content to the change in water potential. In other words, a greater capacitance would allow the plant to lose water with very little change in the water potential of the tissues. Increasing the amount of water storage capacity by larger trees has been proposed as a compensatory mechanism for hydraulic limitations in large trees (e.g., Phillips et al. 2003). The stored water does not need to pass through all the conductive system when it is transpired. Therefore, the increase in capacitance may allow larger trees to transpire more

water, avoiding some of the frictional resistance to water flow. The use of stored water, then, would allow leaves to maintain stomata open for longer periods of time, thus increasing the possibility of carbon gas exchange. Although the measurements of Phillips et al. support the idea of significantly higher capacitance in older trees, the iteration method used in this thesis to estimate the average capacitance per unit leaf area of the stands showed only a small difference between the old-growth and young stands. Therefore, there was no accountable simulated increase in transpiration or GPP due to the increase in capacitance from the young to the old-growth stand. Moreover, when varying the capacitance value beyond the natural variation found between sites, the impact on transpiration was surprisingly small (7% of variation in transpiration when capacitance was varied 200%, holding all other variables constant). The results of this study do not support the hypothesis of capacitance as a mechanism to compensate for hydraulic limitations in old-growth stands. However, no conclusion can be drawn at the individual tree level, where the increase in stored water capacity may partially compensate for the increase in path length.

Leaf area distribution. Little attention has been given to the change in leaf area distribution in the discussion about age-related decline in forest stands. However, the modeling approach of this study showed that the change of the vertical distribution of leaf area (i.e., the foliage distribution in the young stand was predominantly at the canopy tops, whereas in the old stand foliage was

distributed much lower through the canopy space) caused an increase in water use efficiency (13.6%) by increasing GPP (2.3%) and decreasing transpiration (13%). This indicates that the structural change in leaf vertical distribution has a compensatory effect for the hydraulic constrains imposed by the increase in height.

Rainfall partition. The differences in canopy structure between the young and old stand resulted in changes in direct throughfall, and maximum canopy water storage of rainfall (CWS). Sensitivity analyses of these variables showed that the combined effect they had on transpiration and GPP was negligible. However, the modification of CWS and direct throughfall from the young site to the old-growth stand caused a shift in the partition of water among different components of the water budget. The most important predicted change was on the evaporation from wet surfaces on the canopy. Consequently, the old growth stand would have more moisture within the canopy that could support other life forms, and potentially the humidity within the canopy airspace would be higher in the old stand.

Misrepresentations of the Model

There are practical consequences imposed by the level of detail required by the model as input parameters at the stand level. The amount of information needed to get an accurate estimate of some of the variables required to parameterize the model made it impossible to measure these parameters

directly in the field. Therefore, in this thesis, an iterative procedure was used to find an adequate average of certain parameters (i.e., AGLSC) for all the species at the stand level. In other cases (i.e., photosynthetic capacity), measurements on Douglas-fir trees were used. This approach to parameterization, particularly the mixing of variables directly measured for an individual species vs. those calculated or inferred as stand averages, could lead to errors in the predictions of the model as discussed below.

Leaf area should be related to the photosynthetic properties and AGLSC of the different species in order to account for the hydraulic constrains and consequent compensatory changes that each species could have. As the response of photosynthetic parameters to most driving variables (e.g., light, humidity) is not linear, using an average among species present in the stand does not give an accurate estimate of the parameters at the stand level. Moreover, trees of different heights may have different root distribution, and in the "real world", those roots should be related to the canopy layers where the trees of different height put their leaves. As SPA is currently configured, there is no distinction between the root distribution at different layers and the strata in the canopy, which those roots supply. Including a detailed approach relating roots to leaf distribution per species would, also allow future users of the model to test the importance of species composition in the age-related decline in forest stands.

The present version of the model uses the same sand and clay content for all the soil layers. Consequently, the water release curves for the different layers are equal. However, in most situations this is not likely to happen, and soil layers should have different water release curves. In addition, in SPA the litter layer is treated as another soil layer, and the only features that can be modified by the moment is the amount of organic matter, which in the model only affects the heat transfer properties.

The model accounts for differences in the vertical distribution of leaf area, but does not account for the effects of gaps in the forest stand. Gaps are an important trait of mature stands and play an important role in the light regime of understory species.

Conclusions

The SPA model predicted transpiration adequately for both young and old-growth stands. However, the accuracy of the predictions in the old-growth stand varied throughout the growing season.

The model predicted that there would be no change in productivity, although this could be an artifact of the parameterization method. The structure of the model should be changed in order to get accurate predictions of GPP in complex structural ecosystems as the old-growth site analyzed in this study.

The modeling approach of this study showed that the change of maximum height from the young stand to the old-growth stand was the most important variable limiting transpiration and photosynthesis. However, the results of this study do not fully support the hydraulic limitation hypothesis.

Diverse mechanisms for hydraulic compensation were observed. Among them, above-ground leaf specific conductivity and minimum midday leaf water potential threshold showed to be the most important variables compensating for the potential hydraulic constrains imposed by the increase in height. Some other compensatory mechanisms proposed (e.g., increased capacitance with tree size, increased fine root biomass), are likely to act at the tree level, but the effects on transpiration and GPP were negligible at the stand level.

The results of the modeling analyses, did not agree completely with any of the hypotheses suggested to explain the age-related decline in forest productivity. However, the decline in productivity after canopy closure is more likely to be produced by a combination of several interacting factors. On the other hand, model results were consistent with the increase respiration hypothesis.

The modifications made to the SPA model software structure will allow the future users of the program to make automatic sensitivity analysis on multiple scalar variables. The calibration process is now much faster and easier than in the previous version of the program.

The modifications made to the SPA model software interface made the model more accessible to other users. Now, a complete parameterization of the model can be done without having to deal with the Fortran 90/95 programming code.

References

Amthor, J. S. 1994. Scaling CO_2 -photosynthesis relationships from the leaf to the canopy. Photosynthesis Research 39:321–350.

Bachelet, D., R. P. Neilson, T. Hickler, R. J. Drapek, J. M. Lenihan, M. T. Sykes, B. Smith, S. Sitch, and K. Thonicke. 2003. Simulating past and future dynamics of natural ecosystems in the United States, Global Biogeochem. Cycles, 17(2), 1045.

Baldocchi, D. 1992. A Lagrangian random-walk model for simulating water vapor, CO_2 and sensible heat flux densities and scalar profiles over and within a soybean canopy. Boundary-layer Meteorology 61:113–144.

Baldocchi,D. and Vogel, C. 1996. Energy and CO_2 flux densities above and below a temperate broad-leaved forest and a boreal pine forest.Tree Physiology 16, 5-16.

Barford, Cl C. Wofsy, S. C. Goulden, M. L. Munger, J. W. Hammond Pyle, E. Urbanski, S. P. Hutyra, L. Saleska, S.R. Fitzjarrald, D. Moore, K.(2001). Factors Controlling Long- and Short-Term Sequestration of Atmospheric CO_2 in a Mid-latitude Forest . Science 294 :1688-1691

Battaglia, M.. Chapter: Stand age effect on productivity in forests: Representation in models and influence on Net Ecosystem Exchange, in Kirschbaum, M.U.F. and Mueller, R. (2001) Net Ecosystem Exchange. Cooperative Research Centre for Greenhouse Accounting. Pg 50-57.

Binkley, D., Smith, F.W. and Son, Y. 1995. Nutrient supply and declines in leaf area and production in lodgepole pine. Can. J. For. Res. 25:621-628.

Boardman, N. K. 1977. Comparative photosynthesis of sun and shade plants. Annual Review of Plant Physiology 28:355–377.

Bond, B.J. and K.L. Kavanagh. 1999. Stomatal behavior of four woody species in relation to leaf-specific hydraulic conductance and threshold water potential. Tree Physiol. 19:503-510.

Bond, B.J., B.T. Farnsworth, R.A. Coulombe and W.E. Winner. 1999. physiology and biochemistry in response to radiation gradients i varying shade tolerance. Oecologia 1999: 183-192.

Cermak, J., E. Cienciala, J. Kucera and J.-E. Hallgren 1992. Radial ve water flow in trunks of Norway spruce and oak and the response severing. Tree Physiol. 10:367-380.

Chen, J., Falk, M Euskirchen, E. Paw U, K. T., Suchanek, T. H. Ustin B.J., Brosofke, K D., Phillis, N. and Bi, R. 2002. Biophysical cont flows in three successional Douglas-fir stands based on eddy-cc measurements. Tree Pyisiology. 22, 169-177.

?ond et al 1999
Oecologia vol 120

flows in three successional Douglas-fir stands based on eddy-covariance measurements. Tree Pyisiology. 22, 169-177.

Decagon Devices, inc. 2002. ECH2O dielectric aquameter, User's Manual for models EC-20 and EC-10.

Domec, J-C. Gartner, B. 2001. Cavitation and water storage capacity in bole xylem segments of mature and young Douglas-fir trees. Trees 15, 204–214.

Domec, J-C. Gartner, B. 2002. How do water transport and water storage differ in coniferous earlywood and latewood?. Journal of Experimental Botany, 53, 2369-2379.

Knechtenhofer,L.A., Xifra,I.O., Scheinost,A.C., Fluhler,H., Kretzschmar,R. 2003. Fate of heavy metals in a strongly acidic shooting-range soil:small-scale metal distribution and its relation to preferential water flow. J.Plant Nutr. Soil Sci. 166, 84-92.

Farquhar G.D., von Caemmerer S, Berry JA. 1980. A biochemical model of photosynthetic CO2 assimilation in leaves of C3 species. Planta 149, 78-90.

Fessenden, J.E. and Ehleringer, J.R. 2002. Age-related variations in δ13C of ecosystem respiration across a coniferous forest chronosequence in the Pacific Northwest. Tree Pysiol. 22: 159-167.

Field C.B. and Mooney H.A. (1986) The photosynthesis-nitrogen relationship in wild plants. In On the Economy of Plant Form and Function (ed. T. J. Givnish), pp. 25-55. Cambridge University Press, Cambridge.

Gifford, R. 2001. Chapter:Plant respiration in Kirschbaum, M.U.F. and Mueller, R. (2001) Net Ecosystem Exchange. Cooperative Research Centre for Greenhouse Accounting. Pg 38-43.

Granier, A., Evaluation of transpiration in a Douglas fir stand by means of sap flow measurements, Tree Physiol., 3, 309– 320, 1987.

Haefner, J. 1996. Modeling biological systems: principles and applications. Chapman & Hall, New York.

Harley PC, Sharkey TD. 1991. An improved model of C3 photosynthesis at high CO2: Reversed O2 sensitivity explained by lack of glycerate re-entry into the chloroplast. Photosynthesis Research 27, 169-178.

Harley PC, Thomas RB, Reynolds JF, Strain BR. 1992. Modelling photosynthesis of cotton grown in elevated CO2. Plant, Cell and Environment 15, 271-282.

Houghton, J.T., L.G. Meira Filho, B.A. Callander, N. Harris, A. Katterıberg and K. Maskell. 1996. Climate change 1996, The science of climate change. Cambridge University Press, Cambridge, 572 p.

Jackson, R.B. Mooney, H.A. Schulze, E.D.1997. A global budget for fine roots biomass, surface area, and nutrient contents. Proc.Natl. Acad. Sci. Vol.94, 7362-7366.

Jones H.G. and Sutherland R.A. (1991) Stomatal control of xylem embolism. Plant, Cell and Environment 14, 607-612.

Jones H.G. (1992) Plants and Microclimate. Cambridge University Press, Cambridge.

Kavanagh, K.L. Bond, B.J. Gartner, B.L. Aitken, S.N. Knowe, S. 1999. Shoot and root vulnerability to cavitation in four populations of Douglas-fir seedlings. Tree Physiology 19, 31–37.

Kerr,R.A.2001. A little sharper view of global warming. Science 294: 765.

Landsberg J.J., Blanchard T.W. and Warrit B. (1976) Studies on the movement of water through apple trees. Journal of Experimental Botany 27,579-596.

Law, B.E., M. Williams, P.M. Anthoni, D.D. Baldocchi and M.H. Unsworth. 2000b. Measuring and modelling seasonal variation of carbon dioxide and water vapor exchange of a Pinus ponderosa forest subject to soil water deficit. Global Change Biol. 6:613-630.

Lawton, Nair, Pielke and Welch (2001) Climatic impact of tropical lowland deforestation on nearby montane cloud forests.Science 294:584-587.

Lehmkuhl, J. F., Ruggiero, L. F., and Hall, P. A. 1991. Landscape-Scale Patterns of Forest Fragmentation and Wildlife Richness and Abundance in the Southern Washington Cascade Range. Wildlife and Vegetation of Unmanaged Douglas-Fir Forests General Technical Report PNW-GTR-285

Matamala, R.,Gonzalez-Meler,M., Jastrow,J.D.,Norby,R.J.,Schlesinger,W.H. 2003. Impacts of fine root turnover on forest NPP and soil C sequestration potential. Science, vol.302:1385-1387.

Mackay, D.S., D.E. Ahl, B.E. Ewers, S. Samanta, S.T. Gower, and S.N. Burrows. 2003. Physiological tradeoffs in the parameterization of a model of canopy transpiration. Advances in Water Resources, 26(2), 179-194.

Magnani, F., Mencuccini, M. and Grace, J. 2000. Age-related decline in stand productivity: the role of structural acclimation under hydraulic constraints. Plant Cell Envir. 23:251-263.

McDonnell,J.J. 1990. A rationale for old water discharge through macropores in a steep, humid catchment. Water Resour.Res. 26,2821-2832.

McDowell, N., H. Barnard, B.J. Bond, T. Hinckley, R.M. Hubbard, F.C. Meinzer, N. Phillips, M.G. Ryan and D. Whitehead. 2002a. The relationship between tree height and leaf area: sapwood area ratio. Oecologia. 132:12-20.

McDowell, N.G., N. Phillips, C. Lunch, B.J. Bond and M.G. Ryan. 2002b. An investigation of hydraulic limitation and compensation in large, old Douglas-fir trees. Tree Physiol. 22:763-774.

Meinzer F.C. and Grantz D.A. 1991. Coordination of stomatal, hydraulic, and canopy boundary layer properties: Do stomata balance conductances by measuring transpiration? Physiologia Plantarum 83,324-329.

Mosley,M.P. 1979. Streamflow generation in a forested watershed, New Zeland. Water Resour.Res.15,795-806.

Murray,J.D.1993. Mathematical Biology. Springer verlag, Berlin.

Phillips,N., Bond, B.J., McDowell,N.G., Ryan,M.G. 2002. Canopy and hydraulic conductance in young, mature and old Douglas-fir trees. Tree Phys. 22:205-211.

Phillips, N.G., Ryan, M.G., Bond, B.J., McDowell, N.G., Hinckley, T.M. and Cermak, J. 2003. Reliance in stored increases wit tree size in three species in the Pacific Northwest. Tree Phys. 23: 237-245.

Richardson, A.D. Statland,C.B. Gregoire, T.G. in press. Root Biomass distribution under three cover types in a patchy Pseudotsuga menziesii forest in western Canada. Annals of Forest Science.

Reid, D.E. B., Silins,U. and Lieffers, V.J. 2003. Stem sapwood permeability in relation to crown dominance and site quality in self-thinning fire-origin lodgepole pine stands. Tree Phys. 23 : 833-840.

Ryan, M.G. and Yoder, B.J. 1997. Hydraulics limits to tree height and tree growth. Bioscience 47:235-242.

Ryan,M.G. and Waring, R.H. 1992. Maintenance respiration and stand development in a subalpine lodgepole pine forest. Ecology 73:2100-2108.

Ryan MG, D Binkley, JH Fownes, CP Giardina, RS Senock. In press. An experimental test of the causes of forest growth decline with stand age. Submitted to Ecological Monographs (4/03).

Saxton K.E., Rawls W.J., Romberger J.S. and Papendick R.I. (1986) Estimating generalized soil-water characteristics from texture. Soil Science Society of Arnerica Journal 90, 1031-1036.

Schimel, D. S. 1995. Terrestrial ecosystems and the carbon cycle. Global Change Biology 1:77–91.

Scholes, R.J. and Noble, I..R. 2001. Storing carbon on land. Science 294: 1012-1014.

Schulze, E.-D., Cermak J., Matyssek R., Penka M., Zimmermann R., Vasicke F., Gries W. and Kucera J. (1985) Canopy transpiration and water fluxes in the xylem of the trunk of Larix and Picea trees - a comparison of xylem flow, porometer and euvette rneasurements. Oecologia 66,475-483.

Sellers, Dickinson, Randall, Betts, Hall, Berry, Collatz, Denning, Mooney, Nobre, Sato, Field, Henderson-Sellers. 1997. Modeling the exchanges of energy, water, and carbon between continents and the atmosphere. Science 275:502-509.

Shaw, Franklin, Klopatek, Freeman, Bible, Newton, Greene, Murphy, (in press). Ecological setting of the wind river old-growth forest. Ecosystems.

Szeicz G. (1974) Solar radiation in plant canopies. Journal of Applied Ecology 11, II 17-1156.

Thomas, S. C. and Winner W. E. 2002. Photosynthetic differences between saplings and adult trees: an integration of field results by meta-analysis .Tree Physiology 22, 117–127.

Thomas, S.C. and Winner, W.E. 2000. Leaf area index of an old growth Douglas-fir forest estimated from direct structural measurements in the canopy. Can. J. For. Res. 30:1922-1930.

Tyree M.T. and Sperry J.S. (1989) Vulnerability of xylem to cavitation and embolism. Annual Reviews of Plant Physiology and Molecular Biology 40,19-38.

Waring, R.H. and J.F. Franklin. 1979. Evergreen coniferous forests of the Pacific Northwest. Science. 204:1380-1386.

Wastney,M.E. Patterson,B.H. Linares, O.A. Greif, P.C. Boston,R.C. 1999. Investigating biological systems using modeling. Academic Press, London.

Williams, M., Bond, B.J., and Ryan M.G. (2001) Evaluating different soil and plant hydraulic constraints on tree function using a model and sap flow data from ponderosa pine. Plant, Cell and Environment 24, 679-690.

Williams, M., W. Eugster, E.B. Rastetter, J.P. McFadden and F.S. Chapin III (2000) The controls on net ecosystem productivity along an arctic transect: a model comparison with flux measurements. Global Change Biology 6: (suppl. 1) 116-126.

Williams M., Law B.E., Anthoni P.M. and Unsworth M. (2001) Using a simulation model and ecosystem flux data to examine carbon–water interactions in ponderosa pine. Tree Physiology 21, 287–298.

Williams, M., Mahli, Y., Nobre, A.E., Rastetter, E.B.,Grace, J. and Pereyra,M.G. 1998. Seasonal variation in net carbon exchange and evapotranspiration in a Brazilian rain forest:a modelling analysis. Plant, Cell and Environment, 21, 953-968.

Williams, M., Rastetter, E.B.. Fernandes, D.N. Goulden M.L,.Wofsy, S.C Shaver, G.R. Melillo, J.M. Munger, J.W.. Fan S.-M and Nadelhoffer K.J.. 1996. Modelling the soil–plant–atmosphere continuum in a Quercus–Acer stand at Harvard Forest: the regulation of stomatal conductance by light, nitrogen and soil/plant hydraulic properties. Plant Cell Environment . 19:911–927.

Wirıner., W. E., Berry, J., Bond, B.J., Cooper, C., Hinckley, T., Ehleringer, J., Fessenden ,J., Lamb, B., McCarthy, S., McDowell, N., Phillips, N., Thomas, S. C., Williams, M.(in press). Canopy Carbon Gain and Water Use: Analysis of Old Growth Conifers in the Pacific Northwest. Ecosystems.

Wullschleger SD. 1993. Biochemical limitations to carbon assimilation in C3 plants – A retrosprective analysis of the A/Ci curves from 109 species. Journal of Experimental Botany 44, 907-920.

Yoder BJ, Ryan MG, Waring RH, Schoettle AW, Kaufmann MR (1994) Evidence of reduced photosynthetic rates in old trees. Forest Science 40:513-527.